Aslak Einbu

Characterisation of Chitin and a Study of its Acid-Catalysed Hydrolysis

Thesis for the degree of philosophiae doctor

Trondheim, April 2007

Norwegian University of
Science and Technology
Faculty of Natural Sciences and Technology
Department of Biotechnology

NTNU
Innovation and Creativity

NTNU
Norwegian University of Science and Technology

Thesis for the degree of philosophiae doctor

Faculty of Natural Sciences and Technology
Department of Biotechnology

ISBN ISBN 978-82-471-1626-5 (printed ver.)
ISBN ISBN 978-82-471-1643-2 (electronic ver.)
ISSN 1503-8181

Theses at NTNU, 2007:74

Printed by Tapir Uttrykk

Characterisation of Chitin and a Study of its Acid-Catalysed Hydrolysis

Aslak Einbu

A thesis submittet in partial fulfillment
for the requirements for the academic title

Ph.D.

Department of Biotechnology,
Faculty of Natural Science and Technology,
Norwegian University of Science and Technology

Trondheim
January 2007

ACKNOWLEDGEMENTS

The work presented in this thesis has been carried out at the Norwegian Biopolymer Laboratory (NOBIPOL), Department of Biotechnology at NTNU, Trondheim.

My supervisor Professor Kjell Morten Vårum is thanked for his guidance, and for introducing me to the field of chitin and chitosan. Olav Smidsrød and Kurt I. Draget are also thanked for supervising parts of my work.

I highly appreciated the warm hospitality and guidance of Professor Tamo Fukamizo and his co-workers during my work on purification of chitinases at Kinki University in Nara, Japan 2003. Unfortunately, the resulting publication on chitinases from zooplankton did not become part of my final thesis.

I wish to thank my co-authors and my colleauges for creating a pleasant working atmosphere and for sharing their knowledge. Odd Inge Optun and Finn Aachmann are thanked for useful discussions and technical assistance in the NMR-laboratory. Mildrid Myhr is thanked for her skillful technical assistance in the lab. She was my often needed mentor and a motivator during my work.

Financial support has been granted by the Norwegian Research Council through the CALANUS project (Grant 143184/140), NOBIPOL and the Department of Biotechnology.

Last but not least, I would like to thank Kari and my family, for love and support.

SUMMARY

Chitin is one of the most abundant biopolymers in nature and the most widespread amino-polysaccharide. Chitin is used as a raw material for the industrial production of chitin-derived products such as chitosans, derivatives of chitin/chitosan, oligosaccharides and glucosamine (GlcN). The main industrial sources of raw material for the production of chitin are cuticles from various crustaceans, mainly crab and shrimp.

The chemical composition of shrimp shells from deep water shrimp harvested industrially in the Barents Sea was studied in relation to the use of shrimp shells as a raw material for chitin production. No clear seasonal variations were found in the content of the three main components of the shell (protein, minerals and chitin). The average chitin content was 18±2 % of the dry weight of the shrimp shells. No significant seasonal variation was found in the molecular weight of the chitin extracted from the shells using an optimised procedure for chitin extraction. This indicates the chitin producers can rely on shrimp shell waste as a stable raw material for chitin production throughout the whole year.

Concentrated and deuterated hydrochloric acid (DCl) was found to be a suitable solvent in order to characterise the chemical composition (F_A) of chitin by ^{1}H-NMR-spectroscopy. In chitin samples extracted from shrimp shell using 1 M NaOH at 95°C for 1-24 hours as the deproteinisation step, F_A was found to decrease linearly with time from 0.96 to 0.91 during the isolation procedure. Extrapolation to zero time suggests that chitin from shrimp shell has a F_A of 0.96, i.e. contains a small but significant fraction of de-*N*-acetylated units.

New methods were developed for the determination of the intrinsic viscosity and the molecular weight of chitin dissolved in alkali. Chitin samples of different molecular weights (produced by heterogeneous acid hydrolysis) were dissolved in alkali (2.77 M NaOH), and their determined molecular weights (from light scattering) were related to intrinsic viscosity by the Mark-Houwink-Sakurada equation, which was found to be

$[\eta] = 0.10 M_w^{0.68} (\mathrm{ml/g})$. Our study of the solution properties showed that alkali is a good solvent to chitin and that the chitin molecules behave as random coils in this solvent. Alkali is an attractive alternative to previously described solvents to chitin, where aggregates and a more extended chain conformation have been observed.

^{1}H-NMR-spectroscopy was used to study the de-*N*-acetylation of the chitin monomer *N*-acetylglucosamine (GlcNAc) and the depolymerisation of the chitin dimer (GlcNAc-GlcNAc) in DCl. A glucofuranosyl oxazolinium ion was found to exist in equilibrium with GlcNAc in acid concentrations above 6 M. The H-1 resonances from the oxazolinium ion can be used to quantify the amount of GlcNAc in a sample of chitin oligomers in DCl. The reaction rate constants for hydrolysis of the glycosidic linkage of the chitin dimer (k_{glyc}) and the *N*-acetyl linkage of the monomer GlcNAc (k_{acetyl}) were determined as a function of acid concentration (3-12 M) and temperature (25-35°C). The two rate constants were found to be similar at the lowest acid concentration (3 M), while k_{glyc} was much higher than k_{acetyl} at the highest acid concentration (12 M). The activation energies of the de-*N*-acetylation and depolymerization reactions were similar at all acid concentrations. This implies that the acid concentration but not the temperature can be used to control k_{glyc} relative to k_{acetyl} during acid hydrolysis of chitin.

The kinetics of the hydrolysis of the chitin and chitosan tetramer ($GlcNAc_4$ and $GlcN_4$) in concentrated HCl was studied using gel filtration to determine the amounts of tetramer, trimer, dimer and monomer as a function of time. A new theoretical model for the kinetics of the depolymerisation of a tetramer was developed. The model uses two different rate constants for the hydrolysis of the glycosidic bonds in the oligomers, assuming that the glycosidic bond next to one of the end residues are hydrolysed faster than the two other glycosidic linkages. The two rate constants were estimated by fitting model data to experimental results. The results show that the hydrolysis of the tetramers is a nonrandom process as the glycosidic bonds next to one of the end residues are hydrolysed 2.5 and 2.0 times faster as compared to the other glycosidic linkages in the fully N-acetylated and fully N-deacetylated tetramer, respectively. From previous results on other oligomers and the reaction mechanism, it is likely that the glycosidic bond that

is hydrolysed fastest is the one next to the nonreducing end. The rate constants for the hydrolysis of the glycosidic linkages of the fully *N*-acetylated oligomer were found to be 50 times higher as compared to the glycosidic linkages in the fully de-*N*-acetylated oligomer.

A new theoretical model was developed to simulate the kinetics of hydrolysis of chitin in concentrated acid. The model uses three different rate constants; two for the hydrolysis of the glycosidic linkages following an *N*-acetylated or a de-*N*-acetylated sugar unit (k_{glycA} and k_{glycD}, respectively) and one for the de-*N*-acetylation reaction (k_{acetyl}). The three rate constants were estimated by fitting model data to experimental results from ^{1}H-NMR of chitin hydrolysed in concentrated DCl. The rate constant k_{glycA} was found to be 50 times higher as compared to k_{acetyl} and 110 times higher than the rate constant k_{glycD}. ^{1}H-NMR-spectra of chitin in concentrated DCl (40°C) were obtained as a function of time until the samples were quantitatively hydrolysed to the monomer glucosamine. The results show that the initial phase of the reaction involves mainly depolymerisation of the chitin chains, resulting in that almost 90% (molar fraction) of the chitin is converted to the monomer GlcNAc which is then de-*N*-acetylated to glucosamine. Our model predicts (in comparison with our previous results) that the yield of GlcNAc is drastically lowered upon a decrease in the concentration of acid, and/or the F_A of the chitin starting material.

LIST OF PAPERS

1) **A. Einbu** and K.M. Vårum (2004). Structure-Property Relationships in Chitosan. In: *Chemical and Functional Properties of Food Saccharides*. Tomasik, P. (ed.) CRC Press, New York, 217-229.

2) R.S. Hagen Rødde, **Aslak Einbu** and K.M. Vårum (2007). A Seasonal Study of the Chemical Composition of Shrimp Shells obtained from Northern Shrimp (*Pandalus borealis*). *Carbohydrate Polymers* (Submitted).

3) **A. Einbu**, S. Nalum Næss, A. Elgsæter and K.M. Vårum (2004). Solution Properties of Chitin in Alkali. *Biomacromolecules* **5**(5), 2048-2054.

4) **A. Einbu**, and K.M. Vårum (2007). Depolymerization and De-*N*-acetylation of Chitin Oligomers in Hydrochloric Acid. *Biomacromolecules* **8**, 309-314.

5) **A. Einbu**, H. Gradsdalen and K.M. Vårum (2007). Kinetics of Hydrolysis of Chitin/ Chitosan Oligomers in Concentrated Hydrochloric Acid. *Carbohydrate Research* (In Press).

6) **A. Einbu** and K.M. Vårum (2007). Chemical Characterisation of Chitin and its Kinetics of Hydrolysis in Concentrated Hydrochloric Acid. *Biomacromolecules* (Manuscript).

Related paper not included in the thesis:

A. Einbu, P.A. Hamnaberg, T. Fukamizo and K.M. Vårum (2007). Characterisation of Chitin Degrading Enzymes from the Copepod *Calanus finmarchicus*. (Manuscript).

TABLE OF CONTENTS

INTRODUCTION

The Calanus Project

This work forms part of the strategic research program «CALANUS». The project addresses possibilities, constraints and consequences of large scale harvesting of zooplankton from a value chain perspective, including biological, technological, and social aspects. As a main component of the outer skeleton, chitin constitutes about 3 % of the dry-weight of zooplankton (Båmstedt, 1980). The vast amounts of zooplankton present in the oceans, makes it one of the biggest potential sources available for the production of chitin. In relation to fractionation of the zooplankton biomass and its possible utilization as fish feed, our interest has been related to chitin and chitin-degrading enzymes.

Chitin and chitosan chemistry

When working with chitin chemistry, there is often a gradual intersection into the field of chitosan. Chitin and chitosan could be defined by physical parameters rather than chemical ones, as the two terms describe a continuum of copolymers of *N*-acetyl-D-glucosamine and D-glucosamine residues. The following introduction emphasises on chitin, which is distinguished from chitosan by its insolubility in dilute aqueous acid solutions (Roberts, 1992). In order to give a brief introduction to chitosan, the review in Paper 1 is included in the thesis.

1 CHITIN

1.1 Chemical structure

Chitin is a linear polymer of $\beta\,(1 \rightarrow 4)$ linked 2-acetamido-2-deoxy-D-glucopyranose.

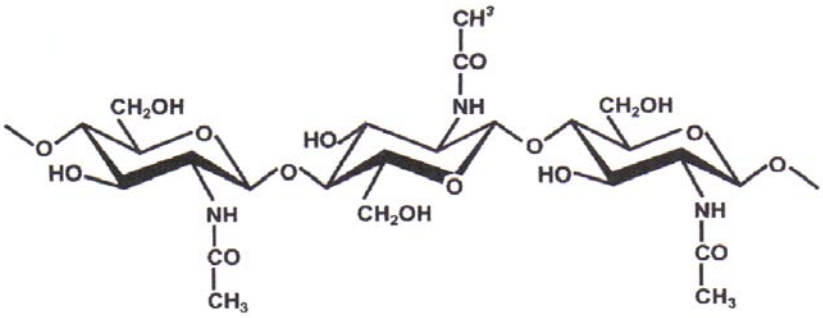

Figure 1.1 Chemical structure of chitin.

Chitin has a resemblance to cellulose both in chemical structure and in biological function as a structural polysaccharide and may be regarded as a cellulose derivative with an acetamido group at carbon 2. Both polymers mainly serve as structural components supporting cell and body surfaces: cellulose strengthens the cell wall of plant cells whereas chitin contributes to the mechanical strength of fungal cell walls and exoskeletons of arthropods (Gooday, 1990).

The idealised chemical structure of chitin as a homopolymer is rarely found in nature, normally there is a limited de-*N*-acetylation, so that the fraction of acetylated units in the polymer (F_A) is between 0.9 and 1.0. This de-*N*-acetylation might be due to the action of chitin deacetylases in chitin-containing organisms, or it may be caused by de-*N*-acetylation during the extraction process (Roberts, 1992).

1.2 Chitin in nature

Chitin is one of the most abundant biopolymers in nature and the most widespread amino-polysaccharide. It is widely distributed in nature in the exoskeleton of all animals with an outer skeleton such as insects and crustaceans. It is also found in microorganisms, e.g. in the cell walls and structural membranes of mycelia of fungi, yeast and green algae (Mathur & Narang, 1990).

During biosynthesis of chitin, monomers of *N*-acetylglucosamine are joined in a reaction catalysed by the membrane-integral enzyme chitin synthase, a member of the family 2 of glycosyltransferases. The polymerisation requires UDP–*N*-acetylglucosamine as a substrate and divalent cations as co-factors. Chitin formation can be divided into three distinct steps. In the first step, the catalytic domain of chitin synthase facing the cytoplasmic site forms the polymer. The second step involves the translocation of the nascent polymer across the membrane and its release into the extracellular space. The third step completes the process as single polymers spontaneously assemble to form crystalline microfibrils of varying diameter and length (Merzendorfer, 2006).

In the chitin crystal structure, the chains form hydrogen-bonded sheets linked by C=O and H-N-groups. In addition, each chain has intramolecular hydrogen bonds between the neighbouring sugar rings: the carbonyl group bonds to the hydroxyl group on C-6. There is also a second hydrogen bond between the OH-group on C-3 and the ring oxygen, similar to that in cellulose (Minke & Blackwel, 1978). This extensive hydrogen bonding shown in Figure 1.2 enhances the stiffness of the chitin chain.

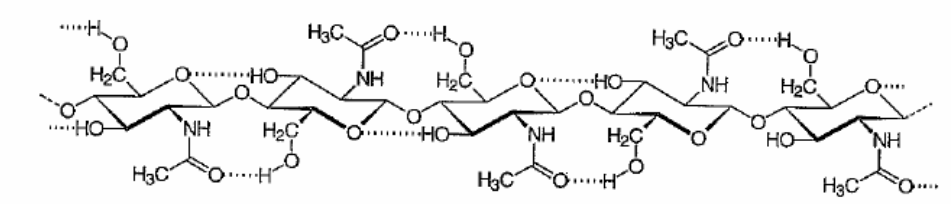

Figure 1.2 Chemical structure of chitin with its intramolecular hydrogen bonds (dotted lines) between the neigbouring sugar rings in chitin (Smidsrød & Moe, 1995)

Chitin has a highly ordered, crystalline structure and has been found in three polymorphic forms, α-, β- and γ-chitin (Hackman and Goldberg, 1965), which differ in the arrangement of the chains within the crystalline regions as shown in Figure 1.3.

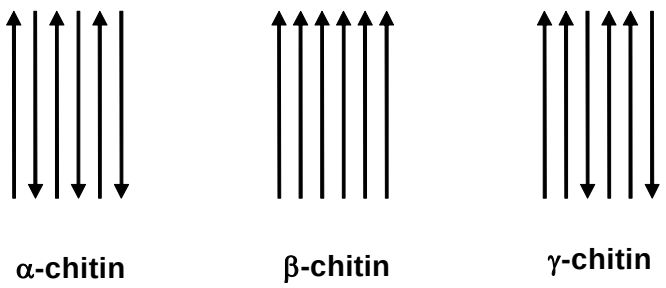

Figure 1.3 Arrangement of the polymer chains in the three forms of chitin.

The three chitin variants differ in their degree of hydration, in their size of the unit cell and in the number of chitin chains per unit cell. α-chitin is the most crystalline and compact form where the chains are arranged in an antiparallel fashion (Carlsstrom, 1957). β-chitin consists of parallel chains, while in γ-chitin two out of three chains are parallel with the third oriented in the opposite direction. The distribution of the polymorphic forms is not related to taxonomy, as different forms may occur in one organism, providing different functional properties: α-Chitin is by far the most abundant form, and is usually found where extreme hardness is required (Rudall & Kenching,

1973). β- and γ-chitin seem to provide toughness, flexibility and motility and may have physiological functions other than support (Muzzarelli, 1977). The poor solubility of chitin is a result of the close packing of chains and its strong inter- and intramolecular bonds among the hydroxyl and acetamide groups (Urbanczyk *et al*., 1997). The inability of α-chitin to swell upon soaking in water is explained by the extensive intermolecular hydrogen bonding (Minke & Blackwell, 1978). On the other hand, β-chitin lacks these interchain hydrogen bonds, and therefore swells readily in water (Blackwel, 1969).

Chitin chains, folded in one of the forms in Figure 1.3, aggregate and form microfibrils in living systems. With only one known exception, the chitin of diatoms (Blackwel *et al*., 1967), chitin is found in nature cross-linked to other structural components. The chitin microfibrils combine with other sugars, proteins, glycoproteins and proteoglycans to form fungal septa and cell walls as well as arthropod cuticles and peritrophic matrices, notably in crustaceans and insects (Kozloff, 1990). In animals chitin is associated with proteins, while in fungal cell wall it is associated with glucans, mannans or other polysaccharides. In fungal walls, it is found covalently bound to glucans, either directly or via peptide bridges (Roberts, 1992). In insects and other invertebrates, the chitin is always associated with specific proteins, with both covalent and noncovalent bonding, to produce the observed ordered structures. There are often also varying degrees of mineralisation, in particular calcification, and sclerotisation involving interaction with phenolic and lipid molecules. In both fungi and invertebrates, varying degrees of deacetylation have been determined, giving a continuum of structure between chitin (fully acetylated) and chitosan (fully deacetylated) (Peter *et al*. , 1986).

The exoskeleton of crustaceans is a noncellular coating, a cuticle secreted by the epidermis. The organic matrix of the cuticle is composed of chitin and associated proteins as seen in Figure 1.4.

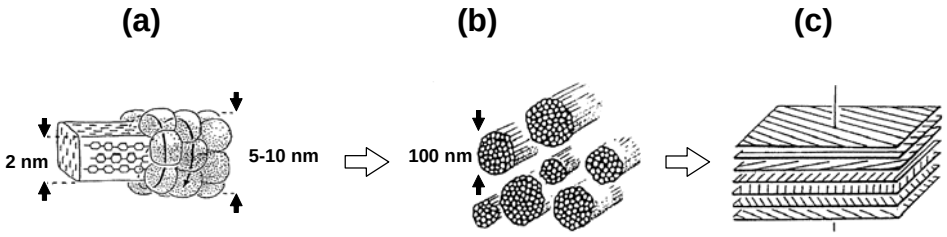

Figure 1.4 Hierarchical levels in the chitin-protein matrix in crustacean cuticles. **(a)** chitin crystals surrounded by proteins. **(b)** Chitin-protein fibrils. **(c)** Schematic representation of fibrils lying horizontal and parallel in successive planes.

In the cuticle, chitin chains are assembled in narrow and long crystalline units. Helically arranged globular proteins are bound to the periphery of these parallel chitin crystals **(a)**. The chitin-protein units are grouped into fibrils of various diameters where the chitin crystals appear as rods semented with proteins **(b)**. The chitin-protein fibrils build up sheets of successive planes of horizontal and parallel fibrils with directions changing from one plane to the other by continuos rotation **(c)**. This structure creates horizontal laminae whose thickness varies from a tenth of a micron to several micrometers (Giraud-Guille, 1998). The new cuticle calcifies after each molt by nucleation and growth of calcium carbonate in the form of calcite crystals. These crystals appear and grow within the fibrillar organic network and ultimately forms into a rigid acellular composite material that forms the exoskeleton (Giraud-Guille & Bouligand, 1995).

1.3 Chitin extraction

Chitin was first isolated in 1811 by the French chemist and pharmacist Henri Braconnot, who extracted chitin as the alkali-resistant fraction from fungi (Braconnot, 1811). Procedures for isolation of high-molecular weight and pure chitin are essential for its use as a raw material to make high quality chitosan. Since chitin is closely associated with proteins, minerals, lipids, and pigments, these components all have to be quantitatively removed to achieve the high purity necessary for biological applications. The common procedure for isolating chitin from crustacean shells involves demineralisation, deproteinisation and decoloration. Minerals in the shells are dissolved using acid while proteins are hydrolysed by alkali. The residues are decolorised using solvents and/or oxidants. Although many methods can be found in the literature for the removal of proteins and minerals, detrimental effects on the molecular weight and F_A cannot be avoided with any of these extraction processes (Percot, Viton & Domard, 2003b). Therefore, a great deal of interest still prevails for the optimisation of the extraction procedure to minimise the degradation of chitin, while at the same time, reducing the impurities down to a level satisfactory for specific applications.

Demineralisation is generally performed by acids including HCl, HNO_3, H_2SO_3, CH_3COOH, and HCOOH, however HCl seems to be the preferred reagent and is applied at a concentration between 0.2 and 2 M for 1-48 h at temperatures varying from 0 to 100 °C. Deproteinisation of chitin is usually performed by alkaline treatments, although other effective reagents have been reported. Typically, raw chitin is treated with approximately 1 M aqueous solutions of NaOH for 1-72 h at temperatures ranging from 65 to 100 °C (Percot, Viton & Domard, 2003a).

An interesting alternative method involves the enzymatic degradation of proteins. However, the residual protein in the produced chitin often remains relatively high and the reaction time is longer compared to chemical deproteination. These drawbacks make the enzymatic method unlikely to be applied on an industrial scale unless progress is made in making the process more efficient (Percot, Viton & Domard, 2003b).

1.4 Commercial applications of chitin

Chitin is mainly used as a raw material to produce chitin-derived products, such as chitosans, chitin/chitosan derivatives, oligosaccharides and glucosamine. An increasing number of useful products derived from chitin continue to attract commercial development. The large number of patents filed involving chitin-derived products reflects the commercial expectations for these products (US Patent and Trademark Office, 2006).

An estimated 75 % of chitin produced is used to manufacture products for the nutraceutical market. Currently the major driving force in the market is the increasing sales of glucosamine as a dietary supplement (Sandford, 2002). Approximately 65% of the chitin produced is converted into glucosamine, ~25% is converted into chitosans, ~9% is used to produce oligosaccharides and approximately 1% goes to the production of *N*-acetylglucosamine (Mustaparta, 2006). Table 1.1 shows estimated world-wide production of chitin-derived products and their market prices (Mustaparta, 2006).

Table 1.1 Estimated global production and market prices of chitin-derived products together with the respective chitin consumption involved in production.

Product	Annual production (tons)	Chitin consumption (tons)	Market price (USD/kg)
Glucosamine	4500	9000	7-35
Chitosans	3000	4000	10-100[a]
Oligosaccharides	500	1000	50-100[b]
***N*-acetylglucosamine**	100	200	20-140[c]

[a] Ultra pure/GMP (Good Manufacturing Practice - Quality System) products can have prices of up to more than 50.000 USD/kg.

[b] Ultra pure and well characterised products can have prices up to more than 10.000 USD/g.

[c] Chemically manufactured: 20 USD/kg and enzymatically manufactured: 100-140 USD/kg.

Variation in the estimated market prices in Table 1.1 depends not only on the quality of the product but also on the amount of product on the market. The main industrial sources of raw material for the production of chitin today are cuticles of various crustaceans,

mainly from crab and shrimp (Kim & Rajapakse, 2005) and the market price is approximately 5-8 USD for average quality chitin (Mustaparta, 2006).

1.4.1 Glucosamine and *N*-acetylglucosamine

2-amino-2-deoxy-D-glucose (glucosamine) and 2-acetamido-2-deoxy-D-glucose (*N*-acetylglucosamine) are the amino sugars that constitute the building blocks of chitin and chitosan. They are found in a variety of naturally occurring molecules, cells and tissues. Figure 1.5 shows the chemical structure of glucosamine and *N*-acetylglucosamine.

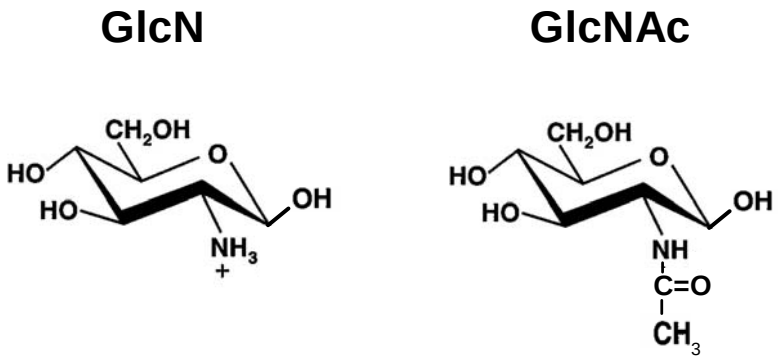

Figure 1.5 Chemical structure of glucosamine (**GlcN**) in its protonated form and *N*-acetylglucosamine (**GlcNAc**).

Glucosamine is commercially prepared from chitin, a process that is mainly performed in concentrated acid (Novikov *et al*., 1997). This process involves two acid-catalysed hydrolysis reactions, i.e. that of the glycosidic linkage (depolymerisation) and that of the *N*-acetyl linkage (deacetylation). Glucosamine products are sold in different salt forms where the most common counter-ions are chloride and sulphate, which depend on the type of acid used during hydrolysis. Currently, China manufactures about 90% of all glucosamine (Sandford, 2002). Glucosamine has been widely promulgated to relieve symptoms in osteoarthritis (Anderson *et al.*, 2005), the most common form of arthritis that can affect the joints, hands, hips, shoulders and knees (see chapter 1.5).

N-acetylglucosamine, which is a minor commercial product, is produced by both chemical acetylation of glucosamine using acetic anhydride (He *et al*., 2001) and by

enzymatic hydrolysis of chitin (Haynes *et al.*, 1999). Enzymatically produced GlcNAc has a higher marked price and is in contrast to chemically produced GlcNAc approved as a food additive in Japan (Mustaparta, 2006).

Even if glucosamine and *N*-acetylglucosamine are currently produced from the chitin from shellfish waste, production could be limited by the amount of raw material available and the product potentially carries the risk of shellfish protein contamination. Currently, work is in progress to develope a new microbial fermentation process on an industrial scale by using strains of *Escherichia coli* modified by metabolic engineering (Deng *et al.* , 2005). Glucosamine and *N*-acetylglucosamine are synthesised in all organisms, including bacteria, yeast, filamentous fungi, plants and animals. In humans, GlcN and GlcNAc are together with glucose the main precursors of the disaccharide units in glycosaminoglycans (such as hyaluronic acid, chondroitin sulfate and keratan sulfate), which are necessary to repair and maintain healthy cartilage and joint function (Mobasheri 2002). Glycosaminoglycans form an important component of connective tissues and may be covalently linked to a protein to form proteoglycans. Figure 1.6 shows the biochemical pathway for the synthesis of glycosaminoglycans in humans.

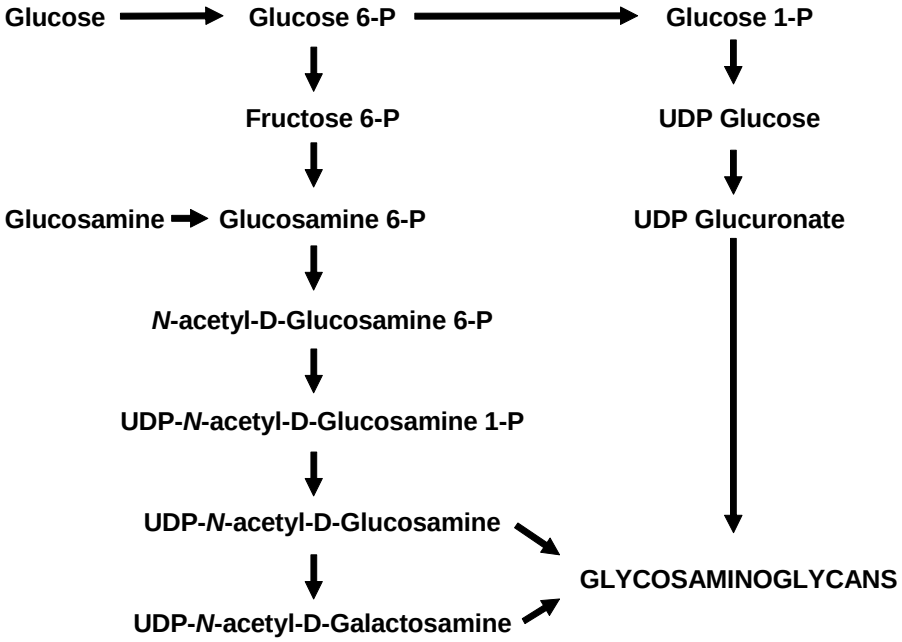

Figure 1.6 The biochemical pathway for the synthesis of matrix glycosaminoglycans in humans (Mobasheri *et al.* 2002).

1.4.2 Chitosan

The term chitosan refers to partially or fully de-*N*-acetylated derivatives of chitin which are water soluble in acidic solutions. Chitosans are a family of linear, binary polysaccharides consisting of $\beta(1 \rightarrow 4)$ linked *N*-acetylglucosamine (**A**-unit) and glucosamine (**D**-unit). A schematic representation of the chemical structure of chitosan is given in Figure 1.7.

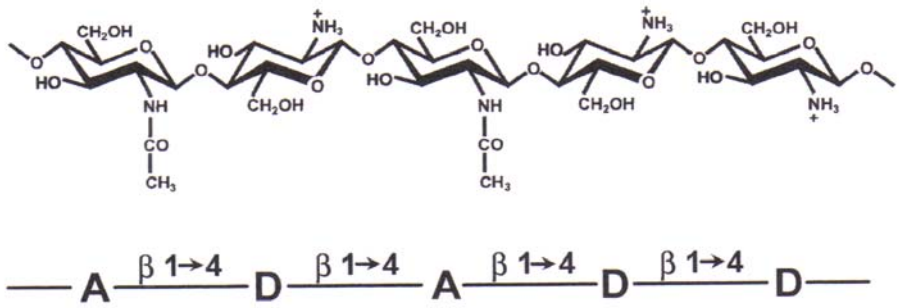

Figure 1.7 Chemical structure of a partially de-*N*-acetylated chitosan.

Industrially, chitosans are normally prepared by alkaline de-*N*-acetylation of chitin (Hirano, 1996). Chitosans prepared by homogeneous de-*N*-acetylation of chitin have been found to have a random distribution of **A**- and **D**-units (Vårum *et al.*, 1991a, Vårum *et al.*, 1991b). Commercial high-molecular weight chitosans with F_A= 0-0.2 are only soluble at pH-values below the apparent pK_a-value of 6.5 of the **D**-units (Anthonsen & Smidsrød, 1995) where the polysaccharide will be highly positively charged. However, high molecular weight chitosans with F_A = 0.4-0.6 have been shown to be fully soluble at neutral pH-values (Sannan *et al*., 1976).

Chitosans are used in dietary supplements, water treatment, food preservation, agriculture, cosmetics, pulp & paper and medical applications (Sandford, 2002). There has been a large increase in chitosan research during the past decade. This is due to its biocompability, biodegradability, non-toxicity, and other unique properties such as film-forming ability, chelation and adsorption properties and antimicrobial activity (Kumar, 2000).

In 2001, the company Primex Ingredients ASA (Norway) promoted its shrimp-derived chitosan as "Self-affirmed GRAS (Generally Recognised As Safe)" under FDA regulations (US Food and Drug Administration). Many had expectations that the affirmation of chitosan as GRAS would open up considerable markets for high-quality chitosans in human consumption. However, the self-affirmation was withdrawn in 2002 (FDA, 2006). Still, it is assumed that the use of chitosan in both biomedical and food applications will increase as the availability of high quality products with defined parameters increases (Sandford, 2002).

1.4.3 Chitooligosaccharides

Chitooligosaccharides are β-1,4 linked homo- or heterooligomers of *N*-acetyl-glucosamine and/or glucosamine. These oligosaccharides can be obtained either by enzymatic or by chemical depolymerisation of chitin or chitosan.

Chitin and chitosan oligosaccharides have been reported to have biological activities such as antimicrobial, antifungal, antioxidant, and immunostimulant effects (Kim & Rajapakse, 2005). The biological activities of chitooligosaccharides depend on both chain length and fraction of acetylated units (Bahrke *et al.*, 2002) together with charge distribution and the nature of the chemical modification (Muzzarelli, 1996).

Unlike chitosan, chitooligosaccharides are readily soluble in water due to their shorter chain lengths and free amino groups in glucosamine units. The low viscosity and the greater solubility of chitooligosaccharides at neutral pH have attracted the interest of many researchers to utilize chitosan in its oligosaccharide form.

1.5 Application of glucosamine for treating osteoarthritis

The increasing sales of glucosamine for treating osteoarthritis is currently the major driving force in the market for chitin-derived products (Sandford, 2002). Approved as a dietary supplement with very few side-effects, glucosamine has become a major commercial product in the US health food market (Hungerford & Jones, 2003). Osteoarthritis, also called degenerative arthritis, results from wear and tear of the joints and is today the most common cause of disability among the elderly in the western world (Clegg *et al.*, 2006). Osteoarthritis is a condition in which low-grade inflammation results in pain in the joints, caused by wearing of the cartilage that covers and acts as a cushion inside joints (Figure 1.8).

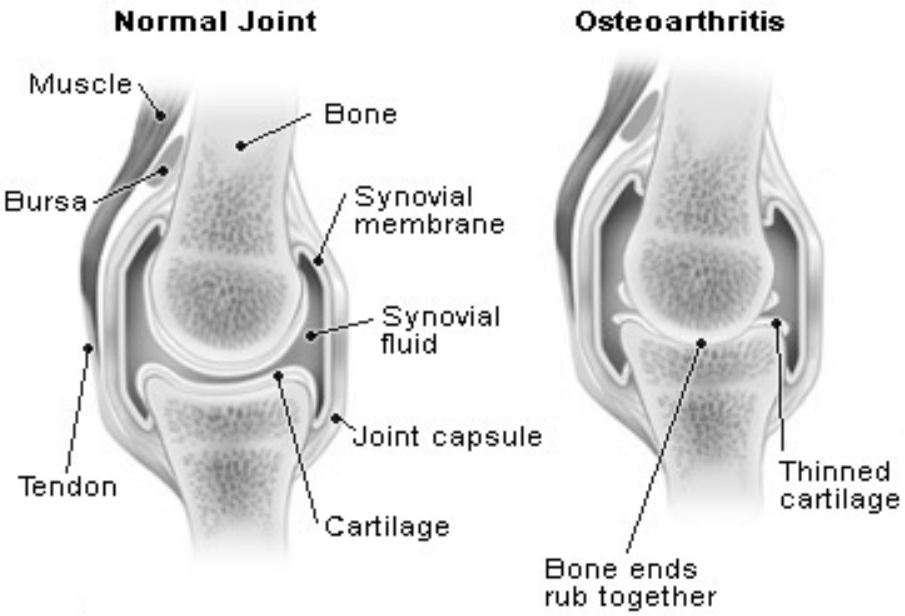

Figure 1.8 Osteoarthritis may affect many different joints of the body, including shoulders, elbows, hands, hips, and knees. (MedlinePlus, 2006).

The symptoms of osteoarthritis ranges from mild discomfort to unbearable pain, which in combination with deformity can cause disability in the joint. Unfortunately there is no cure for osteoarthritis, but the disease can be slowed down and controlled with traditional anti-inflammatory drugs. This short term symptomatic treatment of the disease has major averse effects and might even worsen the osteoarthritic process.

Because of this, there has been a great interest in the search for compounds that may directly interfere with the disease processes and exert more specific effects than the anti-inflammatory and pain-relieving drugs used today.

Glucosamine has been seen by many as a promising alternative for the pharmacological treatment of osteoarthritis. Because of its high concentration in joint tissues, the hypothesis that glucosamine supplements would provide symptomatic relief for osteoarthritis was developed more than 30 years ago (D'Ambrosio *et al*., 1981). Clinical trials with glucosamine for the treatment of arthritis started in the early 1980s. Since then a multitude of studies on the effects of glucosamine as a therapy for treating osteoarthritis have been conducted and it has been increasingly used as a dietary supplement (Hungerford *et al*., 2003). However, there is a conflicting evidence as to its therapeutic effectiveness.

As a constituent of glycosaminoglycans in cartilage matrix and synovial fluid, glucosamine could have various pharmacological actions in cartilage and joint tissues. Studies have shown that orally administered glucosamine is absorbed and distributed to joint tissues, and that it has anti-inflammatory and anabolic properties (Hua *et al.*, 2005; Regnister *et al.*, 2001). Despite these observations, the precise mechanism of action of glucosamine has not been elucidated. Recent studies (Clegg *et al*., 2006) suggest glucosamine does not reduce pain effectively in a sample of patients, however analyses suggest it may be effective in a subgroup of patients with moderate-to-severe knee pain.

The evidence for the effects of glucosamine as a therapy for treating osteoarthritis are conflicting. The future of glucosamine as a commercial product depends on the outcome of the ongoing debate about its effects in the treatment of osteoarthritis.

2 CHARACTERISATION OF CHITIN

Chemical and physical/chemical characterisation of chitin is important both scientifically and with respect to its commercial utilization. However, the aqueous insolubility of chitin limits the methods that are available for its characterisation studies. There is therefore a need to establish new methods to characterise chitin.

The chemical composition (i.e. the fraction of acetylated units) and the molecular weight/molecular weight distribution are the two main characteristics of a chitin sample. In addition, residual protein, moisture content, pigments, ash, lipids, heavy metals and crystal structure can be parameters of interest, depending on the intended use (Roberts, 1992).

2.1 Quantification of chitin

The easiest method to determine the content of chitin in a sample, is by weighing the chitin which can be extracted. This method is especially suitable for samples like crustacean shells and other samples which contain mainly chitin in addition to proteins and minerals. In the case of such chitin sources, the common extraction procedure described in Chapter 1.3 will produce a pure chitin extract representative the chitin-content of the source. The determination of chitin in biological samples is also routinely accomplished by colorimetry of the amino sugars liberated after acid hydrolysis (Gatt & Berman, 1966) This method is especialy suited for handling large numbers of samples. Determination of acetic acid liberated from complete hydrolysis in HCl has also been developed as a method for quantification of chitin (Holan *et al.*, 1980). In this case, however, it is necessary to assume the chitin present is fully *N*-acetylated.

2.2 Crystal structure of chitin

X-ray crystallography is a technique in which the pattern produced by the diffraction of X-rays through the closely spaced lattice of atoms in a crystal is recorded and then analysed to reveal the nature of the lattice. X-ray diffraction of a polysaccharide is a non-trivial task, since many fewer reflections are obtained from a polysaccharide than from a mono- or disaccharide crystal. The structure of chitin, however, has been determined by X-ray diffraction (Darmond & Rudall, 1950; Blackwel, 1969; Minke & Blackwel, 1978). The structure of α-chitin has been investigated more extensively than that of either the β- or γ-form, simply because it is more common (Roberts, 1992).

2.3 Degree of *N*-acetylation of chitin

The search for quick, user-friendly, low cost and accurate methods to determine the degree of *N*-acetylation (F_A) of chitin and chitosan has been of major interest over many decades (Duarte *et al.,* 2002). Another important methodological factor to consider is its suitability to efficiently analyse a large number of samples. This apparently simple analytical problem turns out to be a rather difficult one, which is well illustrated by the extensive number of different techniques. Non-destructive methods have the advantage of avoiding manipulation of the polymer. For destructive techniques such as hydrolysis, pyrolysis or derivatisation, methods of which the consequences are not always well known. F_A and the free amine group content in chitin are inversely related, and the former may be obtained directly by determining the concentration of acetyl groups, or indirectly by determining the amine group concentration.

2.3.1 Hydrolytic methods

F_A of chitin can be determined by different hydrolytic techniques by hydrolysis followed by determination of acetic acid or amino sugars produced (Ng *et al.*, 2006). These methods have no requirement for the sample to be soluble.

2.3.2 Pyrolytic methods

Sato *et al.* (2002) reported on a method for the determination of F_A of chitin and chitosan based on reactive pyrolysis-gas chromatography in the presence of an oxalic acid aqueous solution. The degree of acetylation could be determined from chromatography of the characteristic products of thermal decomposition of chitin in the absence of oxygen.

2.3.3 IR spectroscopy

Infrared spectroscopy can be used to investigate the composition of a chitin sample (Moore & Roberts, 1977). Due to its simplicity, relative instrument availability, and independence of sample solubility, IR spectroscopy is one of the most studied methods for characterisation of chitin and chitosan (Ng *et al.*, 2006). Infrared spectroscopy offers the possibility to measure different types of interatomic bond vibrations at different frequencies. The analysis of IR absorption spectra allows insight into what type of bonds are present in the sample. In order to analyse a sample, a beam of infrared light is passed through the sample, and the amount of energy absorbed at each wavelength is recorded. Although the best results are obtained from cast films, the method can also be used on insoluble samples. The IR spectrum of α-chitin shows two absorption bands at approximately 1655 and 1625 cm^{-1}, characteristic of hydrogen bonded amide groups. The F_A of a chitin sample can be determined by the ratios of different IR absorption bands, as these bands disappear upon deacetylation of the sample (Baxter *et al.*, 1992). Due to the different intra- and intermolecular hydrogen bonds in chitin, there is a statistical mixture of orientations from groups forming inter- or intramolecular hydrogen bonds. As a result the chitin structure contains two types of amide groups, which differ in their hydrogen bonding, and account for the splitting of the amide band in the infrared spectrum (Minke & Blackwell, 1978).

2.3.4 NMR-spectroscopy

NMR is one of today's most powerful tools in the study of polysaccharide composition and sequential structure. NMR is a non-destructive method resulting in retained structure and conformation of the polysaccharide, making it possible to monitor reactions and other structural and physical properties under different solvent conditions.

Due to its insolubility in most solvents, little work has been performed on chitin using aqueous-state NMR. However, several articles have been published on the solid-state NMR of chitin. High-resolution ^{13}C Cross-Polarisation Magic-Angle Spinning (CP-MAS) NMR spectra have been reported for a variety of solid chitin samples (Saito *et al.*, 1982, Duarte *et al.*, 2001). Combined with high-power ^{1}H decoupling (HPDEC) during the acquisition period, this method considerably increases the sensitivity of ^{13}C NMR, and the degree of deacetylation of chitin may be readily determined. Determination of chemical composition of chitin by ^{15}N CP-MAS solid state NMR has also been reported (Heux *et al*., 2000), but due to the lower abundance of this isotope and line broadening effects, ^{15}N NMR is considerably less sensitive than ^{13}C solid-state NMR: detection of acetylation levels lower than 10% is not possible.

Only highly crystalline samples of chitin display narrow line widths compared to the aqueous state NMR-spectra. Solid-state NMR may detect differences between the α- an β- chitin structures, due to the difference in line width in the spectra. It has been reported that in ^{13}C CP-MAS spectra of solid chitin, spectra of α-chitin have broader lines than in spectra of highly crystalline β-chitin (Tanner *et al.*, 1990).

2.3.5 Elemental analysis

Pure chitin with $F_A = 1.0$ has a nitrogen content of 6.89 % while chitosan with $F_A = 0.0$ has 8.69 %. Thus, in theory it is possible to determine the degree of *N*-acetylation from a knowledge of the nitrogen content. However, because of the problems caused by the

presence of moisture, which is difficult to eliminate, and the possible presence of inorganic materials, the use of the Nitrogen/Carbon (N/C) ratio is to be preferred. Pure, protein-free samples are crucial, since the N/C ratio of proteins is considerably different from those of chitin and chitosan (Pelletier *et al.*, 1990).

2.3.6 UV-spectroscopy

UV-spectroscopy is commonly available, but it is limited to the solubility of the sample and the UV-transparency of the solvent. Castle *et al.* (1984) used UV-spectroscopy quantitatively with chitin dissolved in DMAc-LiCl. Although an absorption band attributable to the *N*-acetyl group appeared at 274-278 nm, its intensity was dependent on the age of the solution due to complex equilibriums. Due to this effect, the relationship between concentration and absorbance was not proportional in all cases, and it was concluded that the method was unsuitable for quantitative work. Hsiao *et al.* (2004) used phosphoric acid (85%) as a solvent for determining F_A by UV-spectroscopy. Due to limited solubility, chitinous material with F_A lower than 0.76 could not be analysed by this method.

2.3.7 Dye adsorption methods

The dye adsorption method can be used for both chitin and chitosan samples regardless of solubility, but the diffusive adsorption should be minimal to obtain good results (Maghami & Roberts, 1988).

2.4 Molecular weight of chitin

One of the most fundamental parameters characterising a macromolecule is its molecular weight. Knowledge of the molecular weight of polysaccharides is of general fundamental importance for the understanding of their biotechnological application and

their role in living systems. The limited choice of solvents, and the stability of the solutions formed, are the main problems for molecular weight determination of chitin. Some of the studies carried out on chitin have made use of water-soluble derivatives. Hackman and Goldberg (1974) examined solutions of carboxymethyl chitin and glycol chitin by static light scattering. While such methods have the benefit of enabling aqueous solutions to be used, the preparation process itself will almost certainly cause a reduction in the molecular weight (Roberts, 1992). In addition, the procedure for extraction of the chitin influences the molecular weight of the chitin sample strongly. This is important to consider when comparing the molecular weight of chitins extracted from different sources and with different extraction procedures.

2.4.1 Solution properties of chitin

Chitin can be dissolved only in a few compounds such as alkali, inorganic acids, highly concentrated formic acid, and N,N-dimethylacetamide (DMAc)-LiCl. Solubilisation of chitin in DMAc containing 5 % LiCl appears to be non-degradative (Terbojevich *et al.*, 1988), while acid solubilisation is accompanied by extensive simultaneous depolymerisation.

The molecular weight (M) of a polymer is related to the intrinsic viscosity $[\eta]$ by the Mark-Houwink-Sakurada-equation

$$[\eta] = K \cdot M^a \qquad (1)$$

where *K* and the exponent *a* both are constants for a given well-defined polysaccharide-solvent system (Tanford, 1961). The values of the parameters *K* and *a* depend on both the polymer-solvent system and the temperature (Flory, 1953). The exponent *a* is a polymer conformation parameter that decreases with increasing molecular compactness. Unlike globular proteins, polysaccharides can have a conformation in solution that is difficult to define or determine with precision. Linear polysaccharides in solution may exist in one of three idealized conformations as visualised in “Haug’s triangle” in Figure 2.1.

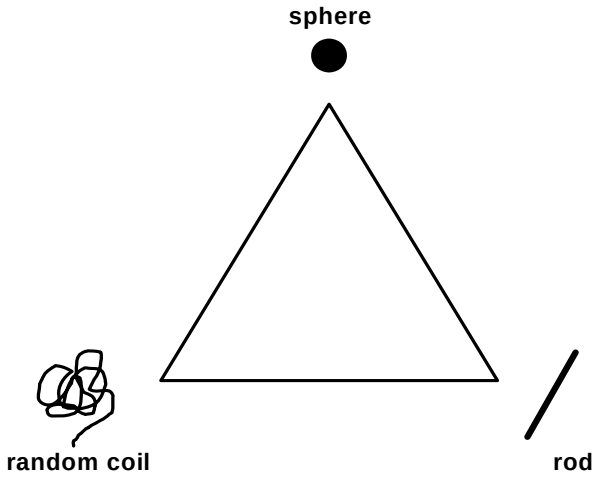

Figure 2.1 Haug's triangle

For extended rodlike molecules, the value of *a* is larger than 1. For random-coil molecules, *a* = 0.5 in a poor solvent and 0.8 in a good solvent. For compact, spherical molecules *a* = 0. Values between 0.5 and 1 are most common for polysaccharides, which is interpreted to a somewhat intermediate between a random coil and a stiff rod conformation. From light scattering and viscosity studies of chitin dissolved in DMAc-LiCl, Terbojevich *et al.* (1988) found the relationship $[\eta] = 0.0024 \cdot M_W^{0.69}$, indicating this solvent enhances the stiffness of the polymer.

Polysaccharides are polydisperse and highly non-ideal in the thermodynamic sense (high exclusion volumes and polyelectrolyte behaviour). For a polydisperse system, the MHS equation yields the viscosity-average molecular weight, M_v . The viscosity average molecular weight is generally closer to the weight average molecular weight, M_w, than the number-average molecular weight, M_n. Therefore, absolute methods yielding M_w (light scattering and sedimentation measurements) should be preferred to those yielding M_n (osmotic pressure measurements and end group determination) in the calibration of the $[\eta]$-M dependency. Once *K* and *a* have been established for a given polymer-solvent system at a specific temperature, the correct M_w of an unknown sample with known $[\eta]$ can be determined. If the polymer in question is polydisperse with

respect to the molecular weight, the unknown sample must have the same molecular weight distribution as the samples used to calibrate the MHS equation. Polysaccharides in solution may also self-associate and form aggregates (Anthonsen *et al.*, 1994), particularly at higher solute concentrations causing an overestimate of the molecular weight average of the single polymer.

3 ACID HYDROLYSIS OF CHITIN

Chitin is known to be one of the most decay resistant of all biomacromolecules. In natural environments, the firm associations with proteins and minerals determine the rates and pathways of degradation (Poulicek *et al.*, 1998). Like other polysaccharides, it can be degraded by many mechanisms, including oxidative-reductive free radical depolymerisation (ORD), alkaline-, enzymatic- and acid-catalysed hydrolysis. Electromagnetic radiation, sonication and mechanical energy have also been reported for the depolymerisation of chitosan (Hai *et al*., 2003).

Hackman (1962) investigated the effect of HCl and other strong mineral acids on the size of the chitin chain, with particular regard to changes occurring under the mild conditions used to prepare “colloidal” chitin. When dissolving chitin at 20°C in concentrated hydrochloric, sulphuric and phosphoric acid, Hackman observed that most of the degradation of the chitin chain occurred during the first few minutes, and that the products formed were oligosaccharides.

Falk and his co-workers found that the rates of formation of acetic acid and glucosamine were the same but initially considerably less than the rate of *N*-acetylglucosamine generation. From this, it was concluded that most of the acetic acid was produced by the hydrolysis of *N*-acetylglucosamine, rather than by hydrolysis of the *N*-acetyl groups in the polymer. Falk also found a maximum concentration of *N*-acetylglucosamine when 50% of the chitin was hydrolysed during acid hydrolysis in 10 M HCl. The authors concluded that good yields of *N*-acetylglucosamine could not be obtained by controlled acid hydrolysis of chitin (Falk *et al.*, 1966).

Holme *et al.* (2001) reported acid hydrolysis to be the primary mechanism involved in the thermal depolymerisation of chitosan chlorides in the solid state and found that the rate of depolymerisation increased with increasing degree of acetylation of the chitosans.

3.1 Acid hydrolysis of the glycosidic linkage

Degradation of polysaccharides occurs via cleavage of the glycosidic bonds. The rate of hydrolysis of the glycosidic linkage is influenced by the ring size of the monomers, configuration, conformation and polarity of the sugar (BeMiller, 1967).

Acid hydrolysis of the glycosidic linkage involves both protonation of the glycosidic oxygen and addition of water to yield the reducing sugar end group. This cleavage of the glycosidic linkage is assumed to be a S_N1 reaction where the rate limiting step is the formation of the activated complex which is a cyclic carbonium-oxonium ion after the protonation. Figure 3.1 illustrates the most accepted reaction mechanism for the acid catalysed hydrolysis of a glycosidic linkage (Edward, 1955).

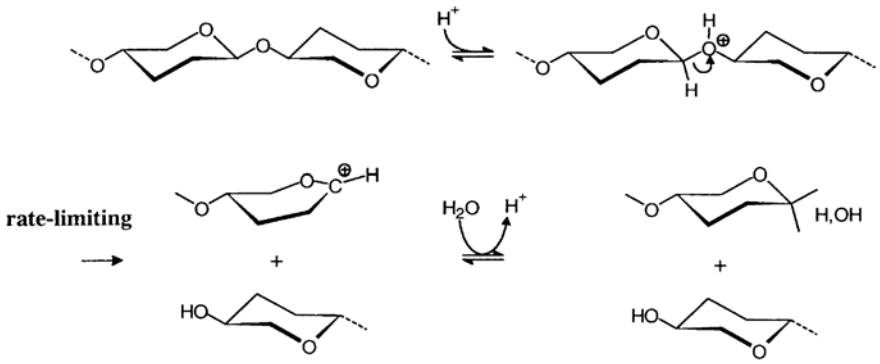

Figure 3.1 Schematic illustration of the proposed reaction mechanism for the acid-catalysed hydrolysis of the glycosidic linkage in chitosans (S_N1 reaction).

The initial step is the protonation of the glycosidic oxygen atom to form the conjugate acid. This is followed by heterolysis of the exocyclic O to C-1 bond to give a cyclic carbonium-oxonium ion which most probably exists in the half-chair conformation having C-2, C-1, O and C-5 in a plane. Reaction with water then gives the protonated reducing sugar, and from it, the reducing sugar is formed.

The acid catalyzed hydrolysis of starch, cellulose and chitosan has been reported to be a non-random depolymerization reaction (Weintraub & French, 1970; BeMiller, 1965;

Vårum *et al.*, 2001). When the calculated amounts of D-glucose and oligosaccharides liberated by the hydrolysis of a given weight of starch or cellulose are compared with the actual amounts formed, it was found that there are more products of low degree of polymerisation and fewer intermediate-sized products than would be expected from a completely random hydrolysis, for any degree or time of hydrolysis (BeMiller, 1965; Purves, 1954). Thus, it appears that acid hydrolysis does not occur by random scission. The non-random acid hydrolysis of polysaccharides can be explained by the reaction mechanism in Figure 3.1, as the glycosidic linkage at the nonreducing end is hydrolysed more rapidly that the other glycosidic linkages in the chain. This conclusion was reached from the fact that hydrolysis of an internal linkage would involve, in the formation of the carbonium-oxonium ion, reorientation of an entire chain; that is, hydrolysis would be diminished by the introduction of a large bulky group, in a manner similar to what has been found for the introduction of various sized groups at C-5 (BeMiller, 1967).

Rupley (1964) studied the acid hydrolysis of chitin in HCl over a range of acid concentrations and temperatures. A high dependency of acid concentration on the depolymerisation of chitin was observed. Rupley suggested the rate of acid hydrolysis was governed by the structure of chitin and claimed the high dependency of acid concentration represented a solvent effect on chain conformation, rather than reflecting the chemical mechanism of hydrolysis. Depolymerisation of chitin should follow first-order kinetics, if all glycosidic bonds were equally reactive. Rupley observed first order kinetics in the process when between 10 to 90% of all glycosidic bonds were hydrolysed. The initial stage proceeded at a slower rate. Rupley speculated that his result might be explained by increased reactivity of the terminal bonds of chitin compared to that of the internal bonds.

In addition, the specificity of the acid-catalysed cleavage of the different chitosan glycosidic linkages in concentrated HCl is such that the linkages between two acetylated units (**A-A**) and between an acetylated and a deacetylated unit (**A-D**) are cleaved at about an equal rate and three orders of magnitude faster than the other two linkages (**D-A** and **D-D**) (Vårum *et al.,* 2001). These differences were explained by the presence of a

positive charge on the **D**-unit under acidic conditions, which makes the protonation of the glycosidic oxygen and the introduction of another positive charge less favourable (Moggridge & Neuberger, 1938). In addition, the neighbouring-group participation where the *N*-acetyl group of 2-acetamido-2-deoxy-β-D-glucopyranose contributes to the stabilisation of the carbonium-ion by forming a oxazoline as an intermediate has been extensively discussed in relation to the mechanism by which chitin, chitin oligomers and derivatives of GlcNAc are hydrolysed (Piszkiewicz & and Bruice, 1967, 1968a,b; Ballardie *et al.*, 1976).

3.2 Acid hydrolysis of the *N*-acetyl linkage

Although amides may in principle be hydrolysed under either acidic or basic conditions, the use of acid hydrolysis in commercial production of chitosan is precluded because of the susceptibility of the glycosidic linkages in chitin to acid hydrolysis. Furthermore, the *trans* arrangement of the C-2 and C-3 substituents in the chitin increases the resistance of the C-2 acetamido group to hydrolysis, so that severe treatments are required to bring about deacetylation (Horton & Lineback, 1965). It is assumed that the acid catalysed cleavage of the *N*-acetyl-linkage is a S_N2 reaction where the rate limiting step is the addition of water to the carbonium ion. Figure 3.2 illustrates the reaction mechanism (Stryer, 1995)

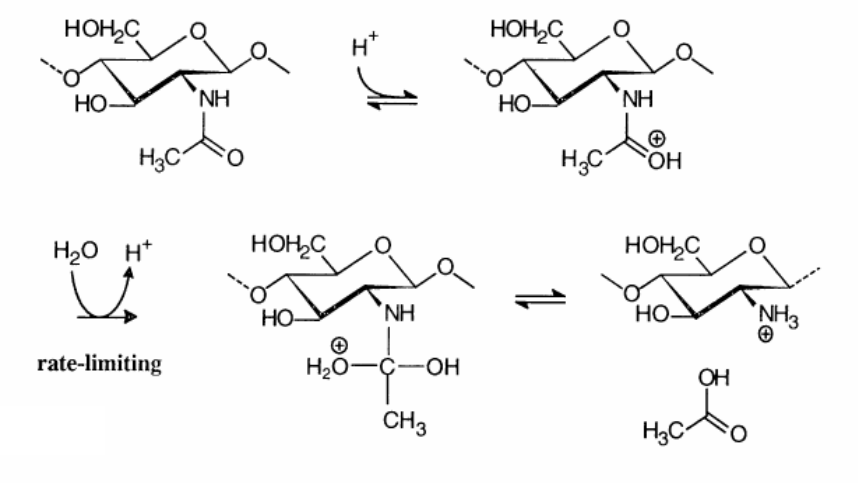

Figure 3.2 Schematic illustration of the proposed reaction mechanism for the acid-catalysed hydrolysis of the *N*-acetyl linkage (S_N2 reaction).

Falk (1966) observed that the formation of acetic acid during hydrolysis of chitin in concentrated HCl was proportional to reaction time, at least during the initial stages of the reaction, independent of the degree of polymerisation of the sample. This result could indicate that the rate of deacetylation is independent of chain length of the *N*-acetylated sugar. Holan and co-workers (1980) found that the rate of reaction for the hydrolysis of the *N*-acetyl-linkage was 10 times higher for *N*-acetylglucosamine than with crystalline chitin. This result was explained by an easier accessibility of the bonds to a deacetylating agent in solution. Holme *et al.* (2001) presented data from solid phase hydrolysis indicating that the *N*-acetyl linkage has a high specificity for reducing ends due to a better availability to the reaction.

Vårum *et al.* (2001) studied the hydrolysis of the glycosidic linkages (depolymerisation) and the *N*-acetyl linkage (de-*N*-acetylation) of partially *N*-acetylated chitosans in dilute and concentrated HCl. While the rate of depolymerization was found to be more than ten times higher than the rate of de-*N*-acetylation in concentrated acid, the two rates were found to be equal in dilute acid. This observation was explained by the difference in water concentration, since the hydrolysis of the *N*-acetyl linkage is an S_N2-reaction where the rate limiting step is the addition of water to the carbonium ion.

3.3 The deuterium isotope effect

The kinetic isotope effect (KIE) is a variation in the reaction rate of a chemical reaction when an atom in one of the reactants is replaced by one of its isotopes. An isotopic substitution will modify the reaction rate when the isotopic replacement is in a chemical bond that is broken or formed. In such a case, the rate change is termed a primary isotope effect. When the substitution is not involved in the bond that is breaking or forming, one may still observe a smaller rate change, termed a secondary isotope effect. Isotope effects are most easily observed when they occur in the rate-determining step of a reaction. Changes in reaction rates are most pronounced when the relative mass change is greatest. For instance, changing a hydrogen atom to deuterium represents a 100% increase in mass, whereas in replacing carbon-12 with carbon-13, the mass increases by only 8%. The rate of a reaction involving a C-H bond is typically 6 to 10 times faster than the corresponding C-D bond, whereas a ^{12}C reaction is only ~1.04 times faster than the corresponding ^{13}C reaction.

The deuterium isotope effect has been found to be of great value in the study of the mechanisms of chemical reactions and in the development of the theories of rate processes. The consequence of the deuterium isotope effect on the reaction rate is dependent on which steps in the reaction deuterium is involved. It has been found that most acid-catalyzed reactions proceed more readily in D_2O than in H_2O. Deuterium oxide has a smaller autoprotolysis constant than water by a factor of 5 and is believed to be less basic than water. Since the concentration of the conjugate acid of the substrate will be higher in D_2O, the rate of the reaction should also be higher in D_2O than in H_2O. Most of the increase in the reaction rate due to the use of D_2O as compared to H_2O as solvent is in the order 1 to 3 times. Therefore, absolute values of rate constants obtained in D_2O can not be directly compared to values obtained in H_2O. In reactions involving two protons, larger effects would be expected than in the cases in which only one proton is involved. In acid-catalysed reactions where the concentration of acid determines which step is the rate-limiting, one should expect the outcome of the isotope effect to be dependent on acid concentration (Widberg, 1995).

3.4 Maillard reaction

Different mechanisms may cause the production of brown colour in solutions of carbohydrates. The Maillard reaction involves amino groups reacting with an aldehyde and can lead to colour change associated with hydrolysis of chitin and chitosan (Pettersen *et al*., 2000). Intensity of browning decreases with an increasing degree of polymerisation of the carbohydrates. In comparison with knowledge about monosaccharides, the reaction behaviour of oligo and polymeric carbohydrates in non-enzymatic browning reactions are hardly known. (Kroh & Schulz, 2001). Even with a significant change in colour of the sample, the substances responsible for colorisation can be present in low concentrations, making them difficult to detect by analytic methods.

SCOPE OF THE THESIS

The scope of this thesis was to develop methods for chitin characterisation and to study the acid catalysed hydrolysis of chitin and chitin oligomers. The papers are discussed in the *Results and Discussion* section according to the following scheme:

Characterisation of chitin

In Paper 2 the seasonal variation of chitin derived from shrimp shells and the chemical composition of shrimp shells were studied (Chapter 4.1). In Paper 3 and 6 we studied chitin dissolved in two different solvents. Paper 6 describes a method for the determination of the chemical composition of chitin by ^{1}H-NMR-spectroscopy of chitin dissolved in DCl (Chapter 4.2). In Paper 3 we studied the solution properties and determined the relationship between intrinsic viscosity and molecular weight of chitin, by using light scattering and viscometric measurements on chitin dissolved in alkali (Chapter 4.3 and 4.4).

Acid hydrolysis of chitin

Chitin oligomers were used as model compounds to study the acid catalysed depolymerisation and de-*N*-acetylation of chitin. In Paper 4, these reactions were studied as a function of acid concentration and temperature (Chapter 5.1). Paper 5 deals with the kinetics of acid hydrolysis of chitin and chitosan tetramers and presents a new mathematical model for the depolymerisation of a tetramer (Chapter 5.2). Based on results from Paper 4 and 5, a new mathematical model for the acid-catalysed hydrolysis of chitin in concentrated hydrochloric acid was proposed in Paper 6 and the model was evaluated using experimental data (Chapter 5.3).

RESULTS AND DISCUSSION

4 CHARACTERISATION OF CHITIN

4.1 A seasonal study of the chemical composition and chitin quality of shrimp shell

In relation the the use of shrimp shell waste products as a raw material for chitin production, the chemical composition and chitin quality of shrimp shells from deep water shrimps harvested in the Barents Sea from January to December were investigated in Paper 2. Shrimps (*Pandalus borealis*) were harvested by seagoing trawlers and frozen within two hours after catch. On land, the frozen blocks of raw shrimps were thawed, steam-boiled and shelled using pilling machines. Representative samples of shrimp shells were taken out and stored at -20° C prior to analysis.

4.1.1 Chemical composition of shrimp shells

Figure 4.1 shows the content of minerals (ash), protein and chitin in shrimp shells harvested during different months given as percentage of dry weight.

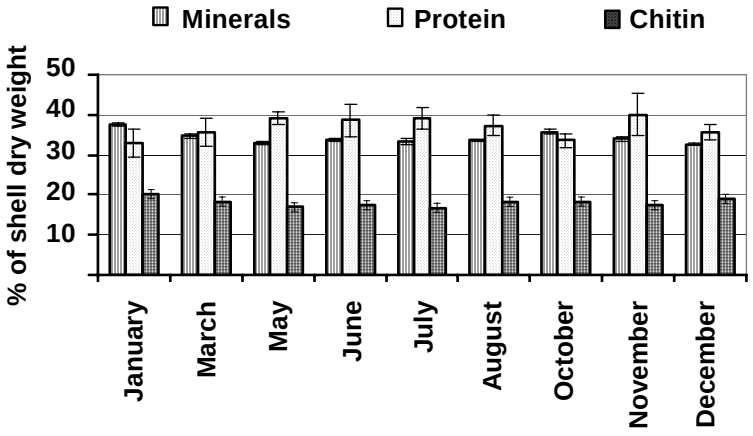

Figure 4.1 Concentration of minerals (ash), total proteins, and chitin in industrially produced shrimp shells given as percentage of dry weight.

The average dry matter content of the shells was 22 ± 2 %, with no significant seasonal variation. The results in Figure 4.1 indicates there is insignificant seasonal variation in the chemical composition of the shrimp shell waste from the shrimp industry. The protein content of the shells was found to vary between 33 to 40 % of the dry weight, with no clear seasonal variation. The chitin content of the shrimp shells was 18 ± 2 % of the dry weight with no significant seasonal variation. The ash content of dried shrimp shells was found to be relatively constant with no seasonal variation (average value 34 ± 2 % of the dry weight). The ash was found to consist of mainly $CaCO_3$. In addition to calcium, Na, Mg and Sr were found to constitute the main ions. Relatively high concentrations of strontium were found in all the samples. The ratio (weight) between calcium and strontium in the shrimp shells was slightly higher to the same ratio in seawater, indicating that calcium is not selectively incorporated into the crustacean shells. The shrimp shells had a low lipid content from (0.3 to 0.5 % of the dry weight) with no significant seasonal variation.

The content of astaxanthin was found to vary from 14 to 39 mg kg^{-1} in our samples of wet shrimp shells. The relative distribution of astaxanthin forms (free, mono- and diester) in the shells suggest a possible conversion from mono- and diester forms to free astaxanthin during storage. The samples stored for the longest time had a generally higher content of free astaxanthin than more fresh ones.

4.1.2 Molecular weight of chitins extracted from shrimp shell

Chitin was extracted from the samples of shrimp shell by an optimised extraction procedure. In relation to the quality of the shrimp shells as a raw material for chitin production, the intrinsic viscosity of the chitin samples were determined by dissolving the chitin in alkali as described by Sannan *et al.* (1977). Molecular weight of the chitins were calculated from the MHS-equation as described in Paper 3 using K=0.1 and a=0.68. Table 4.1 shows the determined intrinsic viscosities with their respective calculated molecular weights.

Table 4.1 Intrinsic viscosities and calculated molecular weights of chitin extracted from shrimp shell dissolved in alkali.

Time of shrimp harvest	Intrinsic viscosity (ml/g)	Molecular weight* (kg/mol)
January	1170	960
March	1160	950
May	1150	940
June	1180	970
July	1250	1060
August	1190	990
October	1250	1060
November	1160	950
December	1200	1000

* Molecular weight determined by the method described in Chapter 4.3.

The molecular weights of the chitin samples varied between 940 and 1060 kg/mol, which can be said to be within the experimental error of ±11 %. Our results indicate that the chitin producers can rely on shrimp shell waste as a stable raw material for chitin production throughout the whole year. Using a common commercial extraction procedure (Percot *et al*, 2001), no significant seasonal variation was found in the molecular weight of extracted chitin.

4.2 Chemical composition determination by ^{1}H-NMR

4.2.1 ^{1}H-NMR-spectroscopy of chitin dissolved in DCl

In Paper 6, the suitability of concentrated and deuterated hydrochloric acid (DCl) as a solvent in order to characterise the chemical composition of the chitin by ^{1}H-NMR-spectroscopy was studied. Chitin can be dissolved rapidly in concentrated acid if it is first wetted with dilute acid. Due to the effect of radiation dampening, the rf-pulses used

had to be significantly longer than the pulses used with water as a solvent. To ensure quantitative uptake parameters, the relaxation times (T_1) of the different protons were determined, using the inversion recovery method. T_1-relaxation times varied between 0.1 and 0.4 seconds, except for the acetate protons, which was found to be significantly longer (2.9 s), as expected.

Figure 4.2 shows a 400 MHz ^{1}H-NMR spectrum of α-chitin dissolved in concentrated DCl at 25° C.

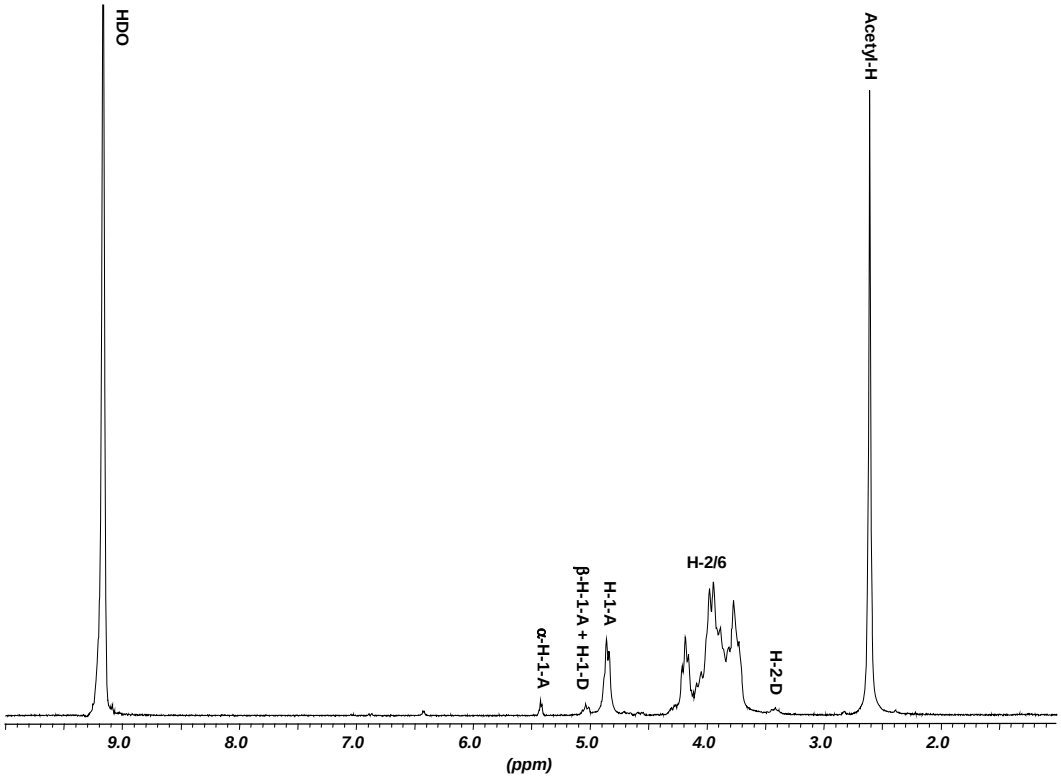

Figure 4.2 ^{1}H-NMR spectrum (400 MHz) of chitin in concentrated DCl at 25°C obtained 30 minutes after dissolution.

The resonances were identified by comparison with spectra of chitin oligomers in the same solvent (see Paper 4). The assignment of the resonances and their chemical shifts (ppm) are given in Table 4.2. One advantage of using concentrated DCl as solvent is that the resonance of the solvent (HDO) does not interfere with any of the carbohydrate protons, as the solvent protons resonate at 9.2 ppm (probably a weighted average of the signals from water and acid protons due to the fast exchange between the two). The

spectra show the characteristic resonances in the anomeric region of the acetylated α- and the β-anomer at 5.43 and 5.05 ppm, respectively. H-1 of internal de-*N*-acetylated units resonate at at 5.07, overlapping with the β-anomeric proton, while H-1 of internal acetylated units resonate at at 4.91 ppm. H-2 of internal de-*N*-acetylated units resonate at 3.44 ppm. Acetyl-protons are found at 2.62 ppm while the remaining ring protons appear between 3.6 and 4.4 ppm. The α- and β-anomer reducing end resonances from a deacetylated unit, which would be expected to appear at 5.65 ppm and 5.21 ppm, are completely absent in the spectrum, since there is no significant de-*N*-acetylation of the sample and due to the specificity of the acid hydrolysis of the glycosidic bonds. Upon de-*N*-acetylation of the sample, the resonance from the protons of acetic acid appears at 2.24 ppm, meaning that any de-*N*-acetylation of the chitin after its dissolution in concentrated DCl can easily be observed and quantified.

^{1}H-NMR spectra of chitin in concentrated DCl can also be used to give an indication of the purity of the chitin sample, as methyl-proton resonances from protein present in the sample would appear between 1.0 and 1.5 ppm.

Table 4.2 Chemical shifts (relative to TSP at 0.00 ppm) of proton resonances for chitin in concentrated DCl at 25°C.

Residue							
	H-1	**H-1 (reducing end)**		**H-2**	**H-2 (reducing end)**	**H-2/6**	**Acetyl-H**
GlcNAc (A)	4.91	5.43	5.05	3.44	3.57 3.32	3.5-4.4	2.62
GlcN (D)	5.07	5.65	5.21			3.5-4-4	

From the identification of the resonances in Figure 4.2, the fraction of *N*-acetylated untis (F_A) of chitin can be determined: The integral representing all H-1 is: $I_{H1A} + I_{H1A+H1D} + I_{H1A}$. By subtracting the integral from H-2 on deacetylated units (I_{H2D}), we obtain the integral representing only acetylated units. Thus, the fraction of acetylated units can be determined from the equation:

$$F_A = \frac{(I_{\alpha H1A} + I_{\beta H1A+H1D} + I_{H1A}) - I_{H2D}}{(I_{\alpha H1A} + I_{\beta H1A+H1D} + I_{H1A})} \quad (2)$$

Figure 4.2 shows there is no significant de-*N*-acetylation of the sample 30 minutes after dissolving the sample in acid. The extent of de-*N*-acetylation of the chitin after 24 hours was determined to only 2 % in concentrated DCl at 25 °C. The uncertainty of the determined value of F_A by this method depends on the precision of the integration of the NMR-spectra. From our spectra, integration of the different resonances could be done with less than 1 % uncertainty, giving a final uncertainty of the determined F_A of about 1.5 %. This illustrates that our method is relatively sensitive and can be used to detect a small decrease in the F_A of chitin.

Concentrated DCl was found to be a suitable solvent in order to characterise the chemical composition of chitin by ^{1}H-NMR-spectroscopy and the fraction of acetylated units (F_A) in the chitin can be determined accurately.

4.2.2 Determination of F_A of chitins from different extraction procedures

In order to evaluate the method for characterisation of F_A of the chitin (Chapter 4.2.1), we analysed samples of chitin extracted at different conditions. When extracting chitin from crustacean shells, the deproteinisation step involving typically 1 M NaOH at elevated temperatures is expected to be more important with respect to de-*N*-acetylation of the chitin upon isolation (Percot et al., 2003). We investigated the time of alkali-treatments of shrimp shells (demineralised by treatment with cold 0.25 M HCl for 35 minutes) by varying the time of treatment with 1 M NaOH at 95°C. The F_A-values of the isolated chitin samples were analysed by ^{1}H-NMR-spectroscopy in concentrated DCl, and the results are shown in Figure 4.3.

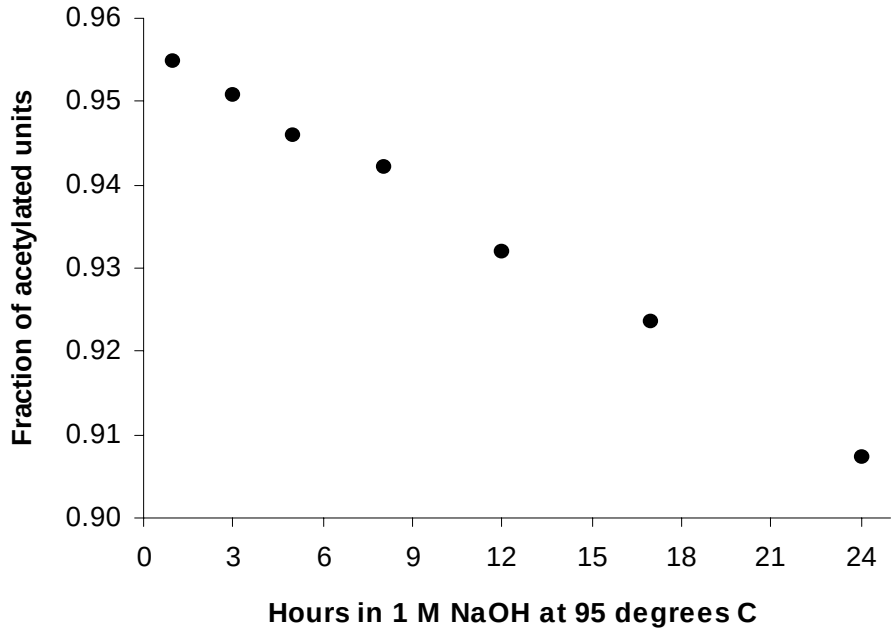

Figure 4.3 F_A-values of chitin samples isolated from demineralised shrimp shells treated with 1 M NaOH at 95°C for 1 to 24 hours.

Figure 4.3 shows that a small but significant deacetylation of chitin occurs upon treatment with 1 M NaOH at 95°C. It should be noted that the samples treated with alkali for less than 5 hours were only partially soluble in concentrated DCl. This was probably due to insufficient deproteinisation, as methyl-proton resonances from proteins was seen in the spectra between 1.0 and 1.5 ppm. Note, however, that extrapolation to zero in Figure 4.3 gives a F_A-value of 0.96, suggesting that the chitin in shrimp shells do contain a small but significant fraction of deacetylated units.

4.3 Molecular weight determination by light scattering

Treatment of an alkaline suspension of chitin with crushed ice yields a solution of alkali chitin in aqueous hydroxide (Sannan *et al.*, 1976). In Paper 3 we studied the solution properties of chitin dissolved in 2.77 M NaOH. Static light scattering was used to determine molecular weights of a series of samples of heterogeneously acid-hydrolysed chitin dissolved in alkali. Molecular weights of the chitin samples were related to intrinsic visocosity by the Mark-Houwink-Sakurada equation.

4.3.1 Chemical stability of chitin dissolved in alkali

To investigate possible de-*N*-acetylation of chitin dissolved in alkali, ^{1}H-NMR was used to determined F_A of a chitin sample which was precipitated after being dissolved in alkali for 8 hours at 20 °C. F_A decreased from 0.91 to 0.85, showing there is a limited deacetylation in the samples of alkali chitin during the time span of our experiments when performing light scattering on samples of chitin dissolved in alkali. To investigate possible degradation of chitin in alkali, the relative viscosity was measured for 8 hours (20 °C), which reflects the time neccesary for preparing a sample and analysing it by light scattering. The relative viscosity of the alkali chitin did not decrease significantly, which indicates no significant change in the molecular weight during this time period.

Chitin samples were dissolved in alkali and the molecular weights of the samples were determined by static light scattering. A Zimm plot of the light scattering data for a typical sample of chitin dissolved in alkali is shown in Figure 4.4.

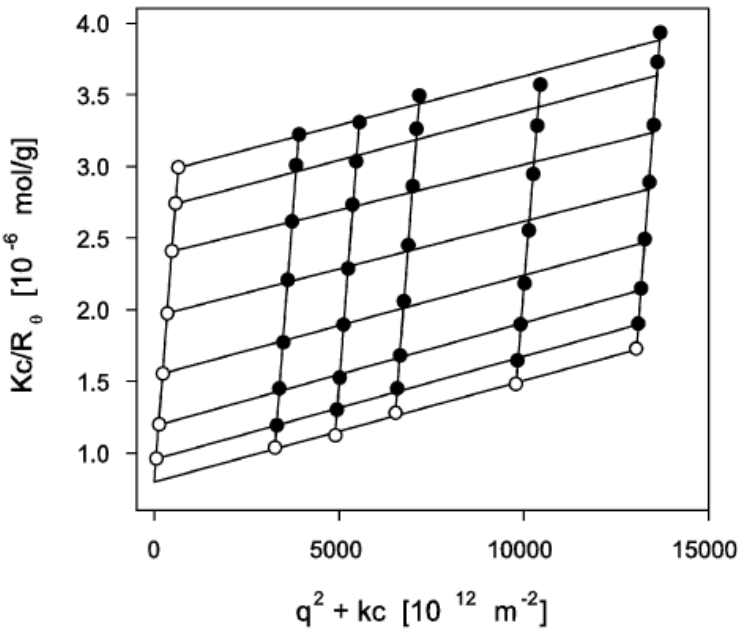

Figure 4.4 Zimm plot for a solution of alkali chitin ([η] = 1350 ml/g). The experimental data are denoted ● , and the extrapolated values are denoted ○.

All Zimm plots gave linear trendlines on extrapolation to zero angle against concentration and to zero concentration against q^2. From these straight lines, the weight-average molecular weight and the second virial coefficient were calculated. Positive second virial cefficients between 1 and 2 x 10^{-3} $mL \cdot mol \cdot g^{-2}$ for all chitin samples indicate that no significant aggregation takes place for the used range of concentrations and that 2.77 M NaOH is a good solvent to chitin.

4.3.2 Preparation of chitin samples with different molecular weight

To prepare chitin samples of different molecular weight, chitin samples were heterogeneously hydrolysed by treatment in 3 M HCl at 25° C for 3, 12, 24, 48 and 345 hours, respectively. Molecular weight averages of the samples were determined by static light scattering of alkali chitin, and was found to be 640, 330, 200, 150 and 100 kg/mol, respectively. The chitin starting material had a molecular weight average of 1200 kg/

mol. Figure 4.5 shows a plot of $(\frac{1}{M_w} - \frac{1}{M_w{}^0})$ versus degradation time of the different chitin samples.

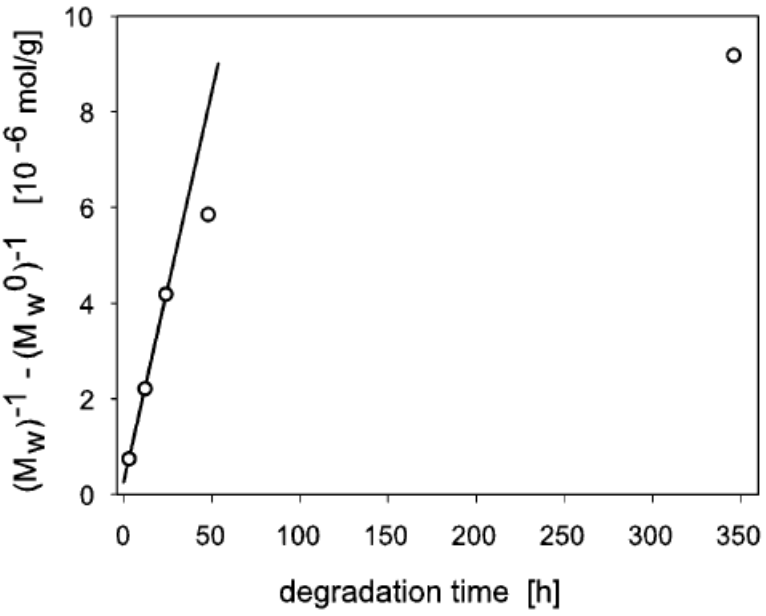

Figure 4.5 Plot of $(\frac{1}{M_w} - \frac{1}{M_w{}^0})$ versus degradation time at 25 °C for the chitin samples in 3 M HCl. The molecular weights were determined by static light scattering measurements of alkali chitin.

A random depolymerisation of the samples would give a linear plot in Figure 4.5, as is the case for the three samples of the lowest degradation time. For reaction times longer than 24 hours, molecular weights deviate significantly from what would be expected from a random degradation. A possible explaination for these results could be that chitin from arthropod outer skeleton consist of both crystalline and amorphous regions, where the amorphous regions are more accessible for acid hydrolysis than the crystalline regions. Even though the degradation is much slower in crystalline regions than in amorphous regions, it will initially appear as random, because of the relatively small number of brooken glycosidic bonds. This may also result in a high-molecular weight fraction of slow degradable crystalline chitin which could appear as aggregates in the sample of alkali chitin. The size distributions of the different chitin samples were obtained from dynamic light scattering of samples of alkali chitin. Figure 4.6 shows the

the equivalent hydrodynamic radius of the samples of different molecular weight in Figure 4.5.

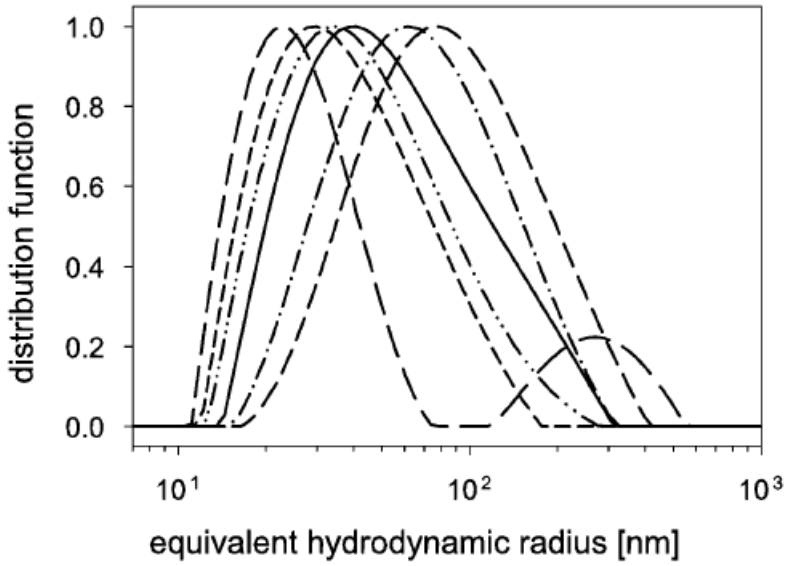

Figure 4.6 The probability density of the equivalent hydrodynamic radius of alkali chitin samples prepared from the chitins of different molecular weight in Figure 4.5. Data obtained by the use of CONTIN on dynamic light scattering results.

The molecular weight distributions move toward lower size with increasing degradation time, as expected. Aggregates ($R_h \approx 300$ nm) are only observed in the sample of the chitin with the lowest molecular weight average. A possible explanation for this is that this sample is the only sample where the aggregates are small enough to pass through the filter used when preparing the sample prior to light scattering.

4.4 Solution properties of alkali chitin

By determining the intrinsic viscosity of the chitin samples of different molecular weight (determined by light scattering), a plot of $[\eta]$ versus M_w (Figure 4.7) was used to determine the parameters *a* and *K* of the MHS equation.

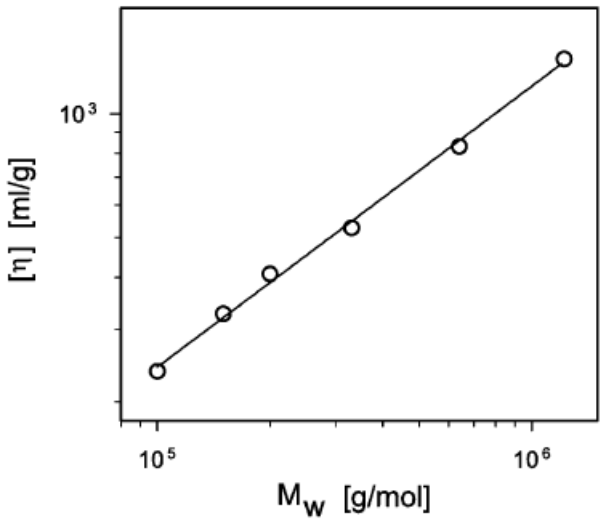

Figure 4.7 Plot of $[\eta]$ versus M_W for chitin solutions prepared from chitin samples of different molecular weight. The experimental data are denoted ○, and the solid line is the regression line.

Parameter *a* was obtained from the slope of this double logarithmic plot. The value *K* was obtained from extrapolation. The Mark-Houwink-Sakurada (MHS) equation was determined to

$$[\eta] = 0.10 M_W^{0.68} (\text{ml/g}) \qquad (3)$$

Having obtained this relationship, the molecular weight of a chitin sample can now be determined by measuring the intrinsic viscosity of the sample dissolved in alkali. The value of exponent *a* = 0.68 in the MHS-equation indicates that chitin dissolved in alkali has a random-coil structure and that the solvent properties are fairly good. The *z*-average radius of gyration, R_g, was obtained from the angular dependency of the scattering intensity at zero concentration. From our data, the radius of gyration can be related to the moleculat weight by the equation

$$R_g = 0.17 M_W^{0.46} (\text{nm}) \qquad (4)$$

Exponent b = 0.46 was obtained from the slope of a double logarithmic plot of radius of gyration, R_g as a function of molecular weight. The value of the exponent in Equation (4) is in agreement with the exponent a of 0.68 in the MHS-equation, which gives further support to the random-coil structure of the chitin molecules in alkaline solutions.

Table 4.3 summarises molecular weight and radius of gyration obtained from light scattering experiments together with the determined number of Kuhn Statistical Segments N_k, the Length of the Kuhn Statistical Segment Q_k, the Contour Length L_c, the Linear Expansion Factor α_S, the Unperturbed Chain Dimension A and the Characteristic Ratio C_∞ of the six different chitin samples prepared by heterogeneous acid hydrolysis. We here assume that the length of a projection of the repeating monomer on the chitin chain is L_{mon} = 0.514 nm and that the molecular weight of this monomer is M_{mon} = 203 g/mol (Terbojevich *et al.*, 1988, Yamakawa & Fujii, 1974, Carlstrom, 1957)

Table 4.3 Number of Kuhn Statistical Segments N_k, the Length of the Kuhn Statistical Segment Q_k, the Contour Length L_c, the Linear Expansion Factor α_S, the Unperturbed Chain Dimension A and the Characteristic Ratio C_∞.

Chitin sample	**M_W [kg/mol]**	**R_g [nm]**	**N_k**	**Q_k [nm]**	**L_C [nm]**	α_S	**A [nm]**	C_∞
C-1	100	38	8.2	30.9	253	1.02	0.29	64
C-2	150	42	14.5	26.2	380	1.03	0.26	51
C-3	200	48	19.5	26.0	506	1.04	0.25	49
C-4	330	60	33.3	25.1	836	1.06	0.24	44
C-5	640	82	65.9	24.6	1620	1.10	0.23	40
C-6	1200	110	132.4	23.3	3089	1.08	0.23	39

Provided that the physical properties are the same along the chain, the Kuhn length (Q_k) should be identical for all samples of the same polymer. From Table 4.3, we observe that Q_k slightly decreases versus M_w. This is in perfect agreement with the fact that the exponent b in Equation (4) equals 0.46 for our chitin samples; that is, chitin is not a perfectly uncorrelated segmented polymer chain. The A and C_∞ values obtained for

chitin in alkali are lower than those of chitin and cellulose in DMAc-LiCl solvent (Terbojevich *et al.*, 1988; *et al.*, 1985). This is as expected, since the DMAc-LiCl is thought to enhance the stiffness of the chitin/cellulose backbone.

Dilute solution properties of chitin in alkali have been determined, showing that alkali is a good solvent to chitin and that the chitin molecules behave as random coils. This solvent system is an attractive alternative to previously described solvents to chitin, where aggregates and a more extended chain conformation have been observed.

5 ACID HYDROLYSIS OF CHITIN AND CHITIN OLIGOMERS

In Paper 4, 5 and 6 we studied the acid-catalysed hydrolysis reactions taking place during acid hydrolysis of chitin in hydrochloric acid. In addition to the general interest in relation to fundamental carbohydrate research, the process of producing glucosamine and *N*-acetylglucosamine by hydrolysis of chitin is of economic interest. By using chitin oligomers as model compounds to study the acid catalysed reactions, we can achieve a better understanding of the process of acid hydrolysis of the chitin polymer.

5.1 Depolymerisation and deacetylation of the chitin monomer and dimer

In Paper 4 we studied the depolymerization and de-*N*-acetylation reaction using the chitin dimer GlcNAc$(1 \rightarrow 4)$GlcNAc and the monomer GlcNAc as model substances, respectively. The reactions were performed in deuterated hydrochloric acid (DCl) as a function of acid concentration (3 to 12 M) and temperature (25-35°C) using ^{1}H-NMR spectroscopy to monitor the reaction rates. The rates of the reactions were determined as a function of acid concentration and temperature and activation energies of the reactions were determined for the different acid concentrations.

5.1.1 ^{1}H-NMR on chitin oligomers in concentrated DCl

The ^{1}H-NMR spectra of the monomer GlcNAc and the dimer GlcNAc-GlcNAc in concentrated DCl (12M) at 25°C were assigned and are shown in Figure 5.1 together with the spectrum of a dimer which had been incubated in concentrated DCl at $25\,^\circ$C for 56 hours.

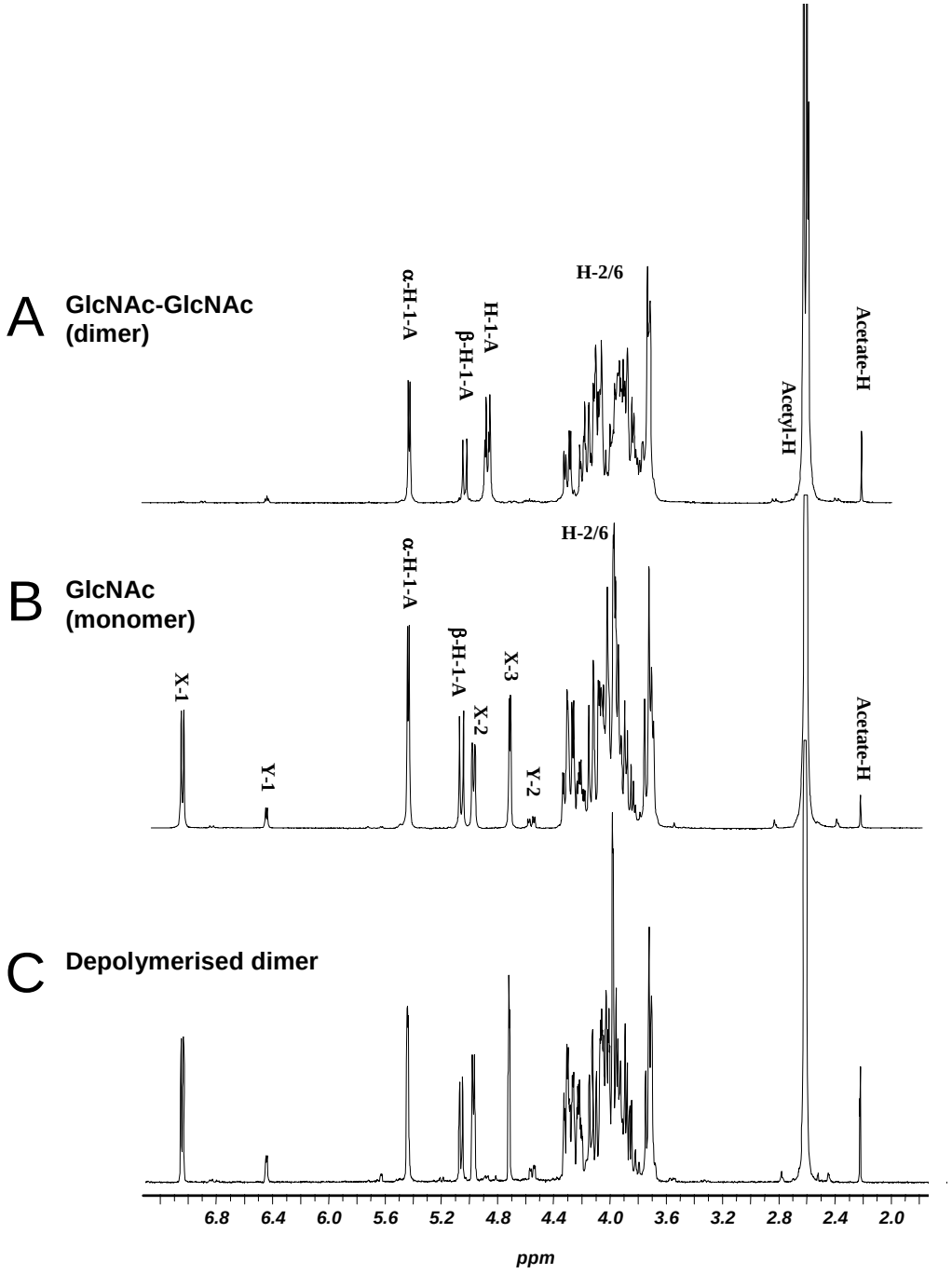

Figure 5.1 ^{1}H-NMR spectra (400 MHz) of GlcNAc and $(GlcNAc)_2$ dissolved in concentrated DCl at 25°C. Chemical shifts are given relative to TSP at 0.00 ppm.

The spectrum of the depolymerised dimer (C) is essentially identical to the spectrum of the monomer (B) in Figure 5.1 with negligible amounts of any de-*N*-acetylated units. The relatively high intensity of the resonance from acetic acid in spectra A and C is due

to acetate present in the commercial sample of dimer (Seikagaku). This shows that all the glycosidic linkages of the dimer GlcNAc-GlcNAc can be hydrolysed without almost any de-*N*-acetylation in concentrated DCl, in agreement with previous results on chitin hydrolysis (Falk *et al.*, 1966).

The spectrum of the monomer GlcNAc contains additional resonances denoted X-1, X-2, X-3, Y-1 and Y-2. The different relative intensities of the resonances indicate they originate from two different compounds (X and Y). Our NMR-data suggest there is a presence of a glucofuranosyl oxazolinium ion existing in equilibrium with GlcNAc in concentrated HCl. The resonances X-1, X-2 and X-3 were assigned to protons 1, 2 and 3 of the glucofuranosyl oxazolinium ion by correlation NMR (^{1}H-^{1}H COSY, HMQC and HSQC) and DEPT 135 of samples of GlcNAc in concentrated DCl (data not shown). H-1 of the glucofuranosyl oxazolinium ion has a relatively high chemical shift at 7.03 ppm, which can be explained by deshielding of the proton by the presence of two electronegative oxygens on each side of C-1. Compound Y is present in lower concentrations than compound X, and we speculate that these resonances may be from the protons of the open ring form of the acetylated reducing end residue of the dimer or of the monomer. The resonances from compund X and Y are not present in spectra of de-*N*-acetylated monomer (GlcN) in the same solvent (spectra not shown). The assumption that compound X is the glucofuranosyl oxazolinium ion is also consistent with the absense of compound X in the spectra of the dimer GlcNAc-GlcNAc, since the conversion of pyranose to furanose requires that C-4 of the reducing end residue is not glycosidically bound.

Figure 5.2 shows the proposed reaction for the formation of the glucofuranosyl oxazolinium ion existing in equilibrium with GlcNAc in concentrated DCl.

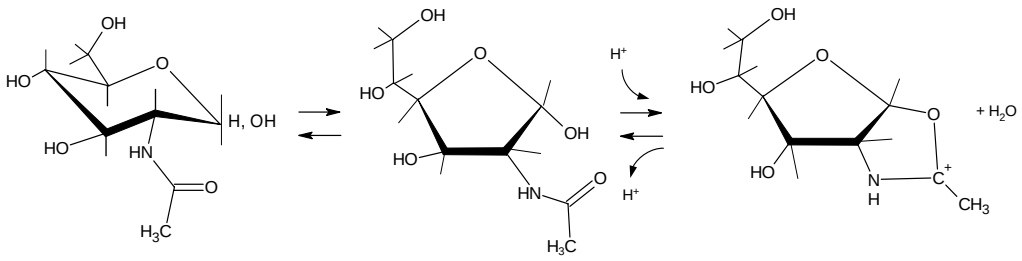

(1) **(2)** **(3)**

Figure 5.2 Proposed reaction for formation of the glucofuranosyl oxazolinium ion (**3**) in concentrated HCl.

Our results indicate it takes approximately 4 hours to establish equilibrium between the glucofuranosyl oxazolinium ion and GlcNAc at 25°C. When equilibrium is established, the concentrations of the oxazolinium ion slowly decreases towards zero due to deacetylation of the sample. Results also show the equilibrium is reversible, as changes in acid concentration of a sample shifts the equilibrium.

^{1}H-NMR spectra of samples of GlcNAc at variyng concentration of DCl were obtained, and a plot of the relative concentrations of the GlcNAc anomers and the glucofuranosyl oxazolinium ion as a function of acid-concentration at equilibrium is given in Figure 5.3.

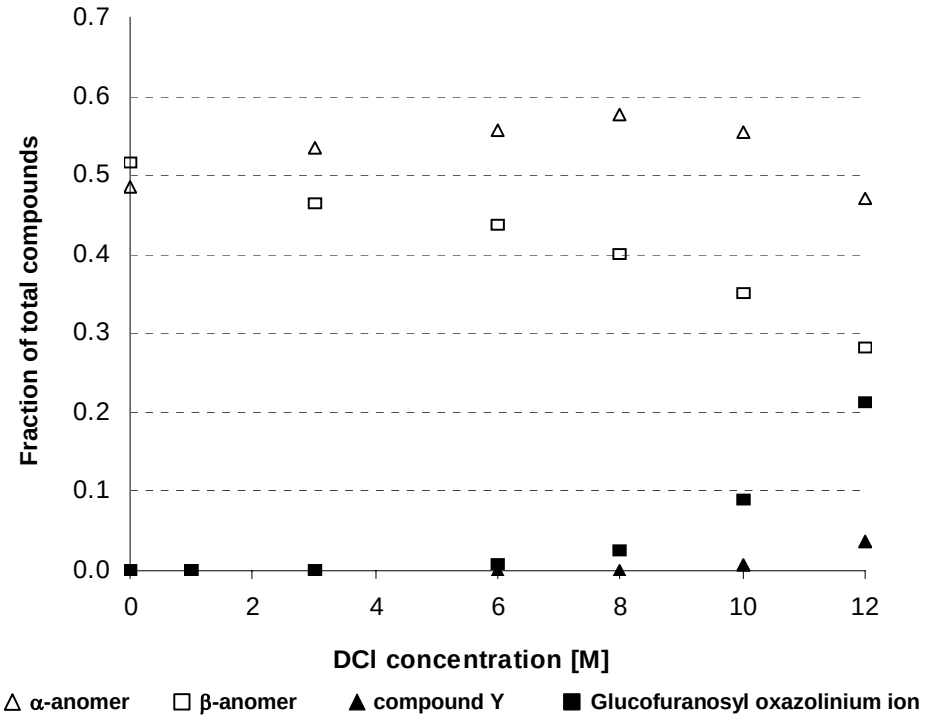

Figure 5.3 Relative concentrations the α- and β-anomers of GlcNAc, the glucofuranosyl oxazolinium ion (compound X) and compound Y as a function of acid concentration.

The relative concentration of compound Y and the glucofuranosyl oxazolinium ion (compound X) decrease with decreasing concentration of DCl, and are below the detection limit when the DCl concentration is less than 6 M.

5.1.2 Rate constants of deacetylation and depolymerisation

By obtaining ^{1}H-NMR spectra as function of time with samples of chitin monomer and dimer in DCl, reaction rate constants of deacetylation and depolymerisation can be determined. The effect of acid-concentration on the rate of the de-*N*-acetylation of the monomer GlcNAc was determined in relation to the reported formation of compound X and Y in Figure 5.3. The results are shown in Figure 5.4.

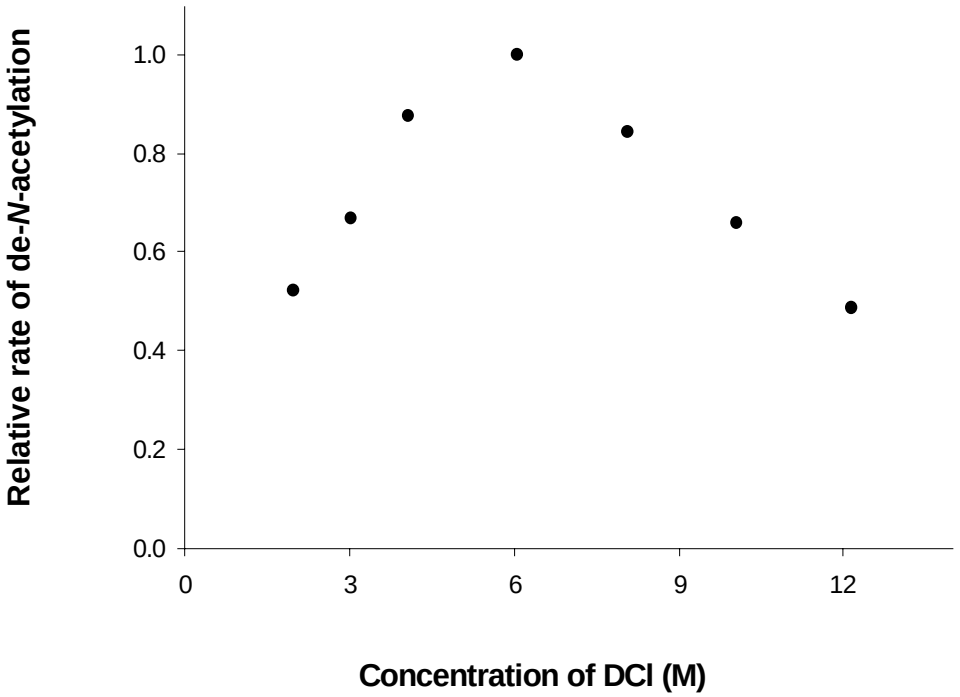

Figure 5.4 Relative rates of de-*N*-acetylation of the monomer GlcNAc as a function of DCl-concentration at 25° C.

The rate of de-*N*-acetylation was found to increase only moderately with increasing acid-concentration from 2 M to ~ 6 M. A further increase in the acid concentration led to a decrease in the rate of de-*N*-acetylation. The formation of the glucofuranosyl oxazolinium ion at DCl-concentrations above 6 M (Figure 5.3) will contribute to a decrease in the concentration of GlcNAc, and the decrease in the rate of de-*N*-acetylation at the higher acid concentrations suggests that the glucofuranosyl oxazolinium ion is not important with respect to the deacetylation reaction. Thus, in a process of preparing glucosamine from chitin, where the deacetylation is the rate-limiting step, the use of HCl-concentrations above 6 M will result in a less efficient formation of glucosamine from deacetylation of *N*-acetylglucosamine.

The rate of de-*N*-acetylation of GlcNAc and the rate of hydrolysis of the glycosidic linkage of the dimer GlcNAc-GlcNAc were determined as a function of temperature at three different acid concentrations (3, 6 and 12 M) and the results are given in Table 5.1,

where k_{acetyl} is the rate constants for the de-*N*-acetylation reaction and k_{glyc} is the rate constants for the cleavage of the glycosidic linkage.

Table 5.1 Rate constants (x 10^8 s), of the de-*N*-deacetylation of GlcNAc (k_{acetyl}) and hydrolysis of the glycosidic linkage in the dimer GlcNAc-GlcNAc (k_{glyc}) as a function of temperature and acid concentration.

	25°C		**30°C**		**35°C**	
	$\boldsymbol{k}_{acetyl}$	$\boldsymbol{k}_{glyc}$	$\boldsymbol{k}_{acetyl}$	$\boldsymbol{k}_{glyc}$	$\boldsymbol{k}_{acetyl}$	$\boldsymbol{k}_{glyc}$
3 M	26	57	53	127	109	250
6 M	39	392	85	819	177	1670
12 M	19	2220	36	4980	71	9430

The reaction rate constant of de-*N*-acetylation of GlcNAc (k_{acetyl}) is about four times higher at 35°C than at 25°C at all three acid concentrations, and k_{acetyl} is found to vary similarly as shown in Figure 5.4 at all three temperatures. Reaction rate constants of hydrolysis of the glycosidic linkage show a 6-fold increase from 3 to 6 M acid-concentration and a further 6-fold increase from 6 to 12 M HCl-concentration, in contrast to the much smaller effect of the acid concentration on k_{acetyl}. This different dependence on the reaction rates of the two reactions with respect to the acid concentration is in accordance with the previously proposed reaction mechanisms (Vårum *et al.*, 2001), where the hydrolysis of the *N*-acetyl linkage was proposed to be a S_N2 reaction while the hydrolysis of the glycosidic linkage was a S_N1 reaction where the rate-limiting step is the formation of the carbonium ion. However, the previous interpretation regarding the rate-limiting step in relation to the water concentration (Vårum *et al.*, 2001) seems misinterpreted, as our current results indicate that the important parameter is the proton concentration.

5.1.3 Activation energies of the de-*N*-acetylation and depolymerisation reactions

The reaction rate constants (Table 5.1) were plotted as a function of the inverse of the absolute temperature (Arrhenius plot) in Figure 5.5.

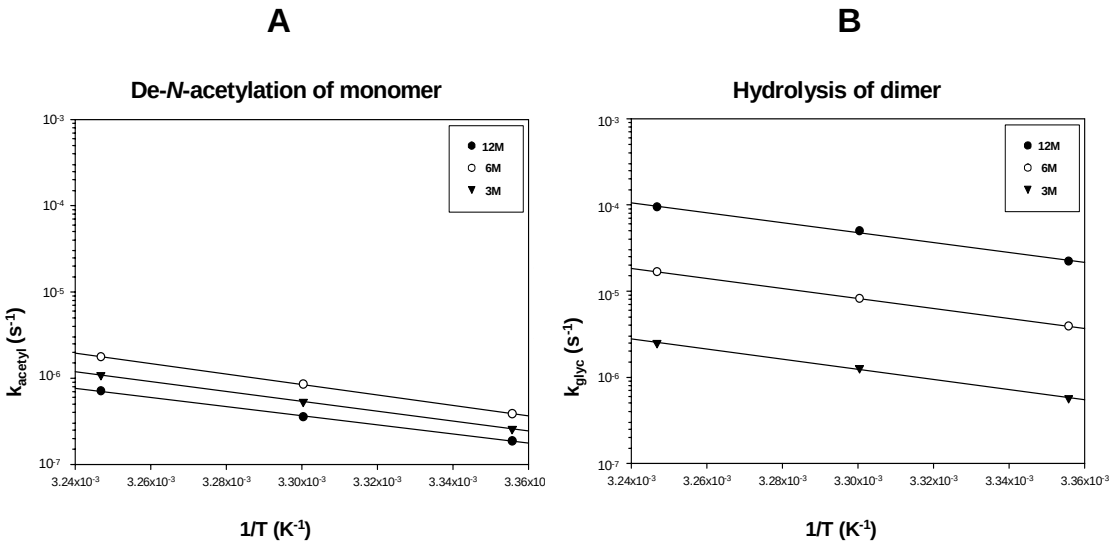

Figure 5.5 Rate constants of de-*N*-acetylation of GlcNAc (**A**) and rate constants of hydrolysis of the glycosidic linkage in the dimer (GlcNAc-GlcNAc) (**B**) (logarithmic scale) as a function of the inverse of the absolute temperature at three different concentrations of hydrochloric acid (Arrhenius plot).

The Arrhenius plots are linear, indicating that the reaction mechanism is the same within the temperature interval tested. There is a relatively small differences between k_{acetyl} as compared to k_{glyc} at the three acid concentrations. Table 5.2 shows the activation energies for de-*N*-acetylation of GlcNAc (E_{acetyl}) and for hydrolysis of the glycosidic linkage in GlcNAc-GlcNAc (E_{glyc}) as determined from the slopes of the trendlines in Figure 5.5.

Table 5.2 Activation energies (kJ/mol) for the *N*-deacetylation (E_{acetyl}) and for the hydrolysis of the glycosidic linkage (E_{glyc}) at different acid concentrations.

		3 M	**6 M**	**12 M**
Activation energy	E_{acetyl}	102 ± 7	116 ± 8	110 ± 8
	E_{glyc}	110 ± 6	111 ± 6	112 ± 4

The values of the activation energies are the same within the experimental error for both reactions and at all three acid concentrations. These activation energies are somewhat higher compared to the activation energies determined for the de-*N*-acetylation of chitin in alkali of 92 kJ/mol (Sannan *et al.*, 1977). The activation energies are similar to that previously reported for acid hydrolysis of the model compound methyl-2-acetamido-2-deoxy-β-D-glucopyranose (in 2.5 M HCl) of 118.4 kJ/mol (Moggridge & Neuberger, 1938). However, the reported activation energy of 94.1 kJ/mol for the hydrolysis of chitin in 11 M HCl (Rupley, 1964) is somewhat lower as compared to the activation energies in Table 5.2. Also, the activation energies for the hydrolysis of the **A-A** and **A-D** glycosidic linkage in chitosans (in dilute acid) of around 130 kJ/mol (Vårum *et al.*, 2001) are higher as compared to the values determined herein, which may be explained by the difference in acid concentrations.

We have found that while the depolymerization reaction increases strongly with increasing acid concentration, the deacetylation reaction is only moderately influenced by the acid concentration. The rate constants k_{acetyl} and k_{glyc} were similar at the lowest acid concentration (3 M). The activation energies of the de-*N*-acetylation and depolymerization reactions were similar at all acid concentrations. Thus, the acid concentration but not the temperature can be used to control k_{glyc} relative to k_{acetyl} when the monosaccharides GlcNAc and GlcN are chemically prepared from chitin in hydrochloric acid.

5.2 Kinetics of the acid hydrolysis of a chitin tetramer

In Paper 5 the kinetics of hydrolysis in concentrated hydrochloric acid of the chitin/ chitosan tetramer ($GlcNAc_4$/$GlcN_4$) were studied and a theoretical model for hydrolysis of the tetramers were compared to experimental results in order to estimate the different reaction rate constants for the hydrolysis of the different glycosidic bonds in the oligomers.

5.2.1 Theoretical model for the hydrolysis of a tetramer

A new theoretical model was developed in order to simulate the kinetics of hydrolysis of the three different glycosidic linkages in the tetramer. The model uses two different rate constants for the hydrolysis of the glycosidic bonds in the oligomers, assuming that the glycosidic bond next to one of the end residues are hydrolysed faster than the two other glycosidic linkages. Figure 5.6 describes the basis of the model, which uses two different rate constants, k_1 and k_2,

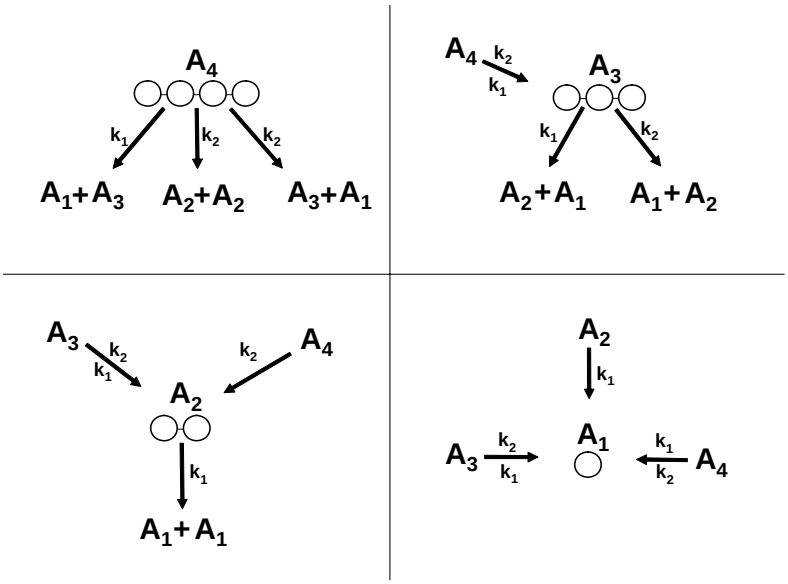

Figure 5.6 Cleavage and formation of the different oligomers starting from the tetramer, A_4 (top left), trimer, A_3 (top right), dimer, A_2 (down left) and monomer, A_1 (down right). The hydrolysis of the glycosidic bonds are described by the rate constants k_1 and k_2.

By solving the four differential equations expressing the formation and cleavage of each of the four oligomers present as seen in Figure 5.6, four equations expressing the molar concentration of tetramer [A_4], trimer [A_3], dimer [A_2] and monomer [A_1] as a function of time and rate constants k_1 and k_2 were obtained (Table 5.3).

Table 5.3 Theoretical model for the hydrolysis of a tetramer. Equations expressing the molar concentrations of tetramer [A_4], trimer [A_3], dimer [A_2] and monomer [A_1] as a function of time and rate constants k_1 and k_2 .

Eq. 1	$[A_4] = e^{-(k_1 + 2k_2)t}$
Eq.2	$[A_3] = \frac{k_1 + k_2}{k_2} \cdot \left(e^{-(k_1 + k_2)t} - e^{-(k_1 + 2k_2)t}\right)$
Eq.3	$[A_2] = \left(1 + \frac{(k_1 + k_2)^2}{2k_2^2}\right) \cdot e^{-k_1 t} - \left(\frac{(k_1 + k_2)^2}{k_2^2}\right) \cdot e^{-(k_1 + k_2)t} - \left(1 - \frac{(k_1 + k_2)^2}{2k_2^2}\right) \cdot e^{-(k_1 + 2k_2)t}$
Eq. 4	$[A_1] = \left(2 + \frac{(k_1 + k_2)^2}{k_2^2}\right) \cdot \left(1 - e^{-k_1 t}\right) + \frac{k_1 + k_2}{k_2} \cdot \left(1 - 2\frac{k_1}{k_2}\right) \cdot \left(1 - e^{-(k_1 + k_2)t}\right) + \left(\frac{k_1 + k_2}{k_1 + 2k_2} - \frac{(k_1 + k_2)^2}{k_2(k_1 + 2k_2)} - \frac{2k_1}{k_1 + 2k_2} \cdot \left(1 - \frac{(k_1 + k_2)^2}{2k_2^2}\right)\right) \cdot \left(1 - e^{-(k_1 + 2k_2)t}\right)$

From Equations 1-4 the theoretical molar fractions of each oligomer can be obtained.

5.2.2 Applying the model on experimental data

The chitin/chitosan tetramers ($GlcNAc_4$/$GlcN_4$) were hydrolysed in concentrated hydrochloric acid at 40 ° C. Neutralised reaction mixtures were separated by gel filtration

and the relative amounts of the different oligomers present during hydrolysis were determined as a function of reaction time.

The theoretical model for molar fractions of each oligomer can be fitted with the molar fractions determined from experimental results to obtain estimates of the rate constants k_1 and k_2. Figure 5.7 shows the molar fractions of the different oligomers during hydrolysis of the fully acetylated chitin tetramer. Theoretical values for the molar fractions are indicated by continuos lines.

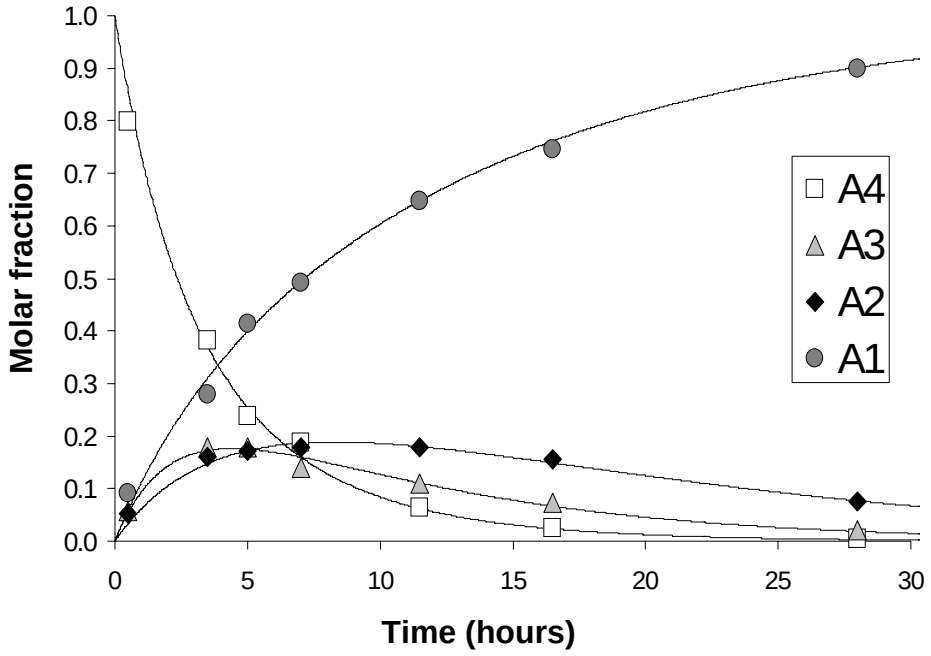

Figure 5.7 Molar fractions of reaction products as a function of time during acid hydrolysis of tetra-*N*-acetylchitotetraose (A4) in concentrated hydrochloric acid at 40 ° C. A4 (tetramer), A3 (trimer), A2 (dimer) and A1 (monomer). Theoretical values for the molar fractions are indicated by continuos lines (Using $k_1 = 2.47 \cdot 10^{-5}\ s^{-1}$ and $k_2 = 1.01 \cdot 10^{-5}\ s^{-1}$).

The determined rate constants k_1 and k_2 show that the hydrolysis of the tetramer is a non-random process, as the glycosidic bonds next to one of the end residues are hydrolysed 2.5 times faster as compared to the other glycosidic linkages in the fully N-acetylated and fully N-deacetylated tetramer, respectively. From previous results on

other oligomers and the reaction mechanism, it is likely that the glycosidic bond that is hydrolysed fastest is the one next to the nonreducing end.

Due to the specificity of the acid catalysed cleavage of the two different glycosidic linkages (**A-A** and **D-D**), the fully de-*N*-acetylated chitosan tetramer was hydrolysed approximately 50 times slower than the acetylated sample under these conditions. During gel filtration, the de-*N*-acetylated monomer, glucosamine, was eluted together with the large salt peak resulting from NaCl from neutralisation of the samples of concentrated HCl. This prevented the integration of the peak resulting from monomer in the chromatogram. Integration was therefore restricted to the peaks from tetramer, trimer and dimer. In order to fit the mathematical model for hydrolysis of tetramer with our experimental results from from hydrolysis of chitosan tetramer, fractions of tetramer, trimer and dimer as a fraction of the sum of all three oligomers were plottet as as a function of time in Figure 5.8**B**. The results from hydrolysis of fully acetylated chitin tetramer (Figure 5.7) was plotted in the same way in order to compare the data from the two reactions (Figure 5.8**A**).

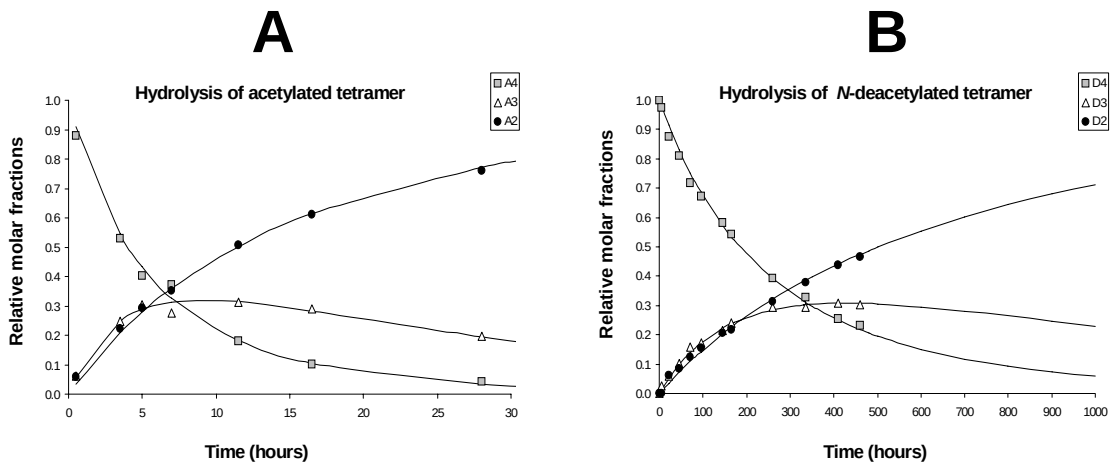

Figure 5.8 Relative molar fractions of tetramer (A4/D4), trimer (A3/D3) and dimer (A2/D2) as a fraction of total tetramer, trimer and dimer as a function of time during acid hydrolysis in concentrated HCl at 40 °C. Hydrolysis of acetylated tetramer (**A**) and de-*N*-acetylated tetramer (**B**). Optimal fitting of the theoretical values for the relative fractions are indicated by continuos lines.

The optimal fit of the theoretical model occurs when the ratio k_1/k_2 is 2.0 and 2.4 for the hydrolysis of de-*N*-acetylated and acetylated tetramer, respectively. These results indicate the hydrolysis is a non-random process for both tetramers; glycosidic bonds next to one of the end residues (probably next to the nonreducing end) are hydrolysed more rapidly than others. Table 5.4 summarises reaction rate constants determined for the two hydrolysis reactions with chitin and chitosan tetramer.

Table 5.4 Estimated reaction rate constants, k_1 and k_2, and the ratio (k_1/k_2) for the hydrolysis of acetylated tetramer and *N*-deacetylated tetramer.

	k_1 (s^{-1})	**k_2 (s^{-1})**	**Ratio (k_1/k_2)**
Hydrolysis of acetylated tetramer (estimate from Figure 5.7)	$2.5 \pm 0.1 \cdot 10^{-5}$	$1.0 \pm 0.1 \cdot 10^{-5}$	2.5 ± 0.3
Hydrolysis of acetylated tetramer (estimate from Figure 5.8)	$2.4 \pm 0.1 \cdot 10^{-5}$	$1.0 \pm 0.1 \cdot 10^{-5}$	2.4 ± 0.4
Hydrolysis of *N*-deacetylated tetramer (estimate from Figure 5.8)	$4.6 \pm 0.2 \cdot 10^{-7}$	$2.4 \pm 0.2 \cdot 10^{-7}$	2.0 ± 0.3

From our results, we can not conclude that the ratio k_1/k_2 for the hydrolysis of the two different oligomers are different, since they can be said to be equal within the experimental errors. The hydrolysis of the glycosidic linkage between two acetylated and two de-*N*-acetylated units is generally accepted to occur via two different mechanism. The different observed rates of hydrolysis can be explained from the mechanism for acid hydrolysis of a glycosdic linkage: For the glycosidic linkage between two de-*N*-acetylated units, the first step of hydrolysis, the protonation of the glycosidic oxygen, proceedes slower since the introduction of a second positive charge near the already protonated de-*N*-acetylated unit is unfavourable. In addition, the *N*-acetyl group of an acetylated unit in the chain is thought to contribute to the stabilization of the carbonium-ion by forming a oxazoline as intermediate giving an anchimeric

stabilization of the positive charge. Since the formation of the carbonium ion is the limiting step in the reaction, this stabilisation makes the hydrolysis more favourable.

However, since the ratio k_1/k_2 is found to be approximately the same for both the acetylated and de-*N*-acetylated tetramer, it seems like the differences in the mechanisms for hydrolysis are not important in relation to the observed rates of the different glycosidic linkages of the oligomers. The observed differences can probably be explained by the most accepted general mechanism for acid hydrolysis: the rate limiting step in the reaction is the formation of a cyclic carbonium-oxonium ion which most probably exists in a half-chair conformation. The hydrolysis of an internal linkage would involve, in the formation of the carbonium-oxonium ion, reorientation of an entire chain while the hydrolysis of a glycosidic linkage next to the nonreducing end-residue would not require reorientation of a bulky group, making it more energetically favourable.

5.3 A study of chitin in concentrated acid by ^{1}H-NMR

In Paper 6 we studied the hydrolysis of chitin in concentrated and deuterated hydrochloric acid (DCl) by solution state ^{1}H-NMR-spectroscopy. A theoretical model was developed to simulate the kinetics of hydrolysis of chitin in concentrated acid.

5.3.1 Theoretical model for acid hydrolysis of chitin

A new mathematical model was developed in order to evaluate the hydrolysis of chitin in concentrated acid. In this model the different sugar units present in the sample are divided into four groups: *N*-acetylated (**A**-unit) or de-*N*-acetylated (**D**-unit) which could each be located at the reducing end ($\mathbf{A_{red}}/\mathbf{D_{red}}$) or as an internal unit ($\mathbf{A_{int}}/\mathbf{D_{int}}$). Figure 5.9 shows a schematic illustration of the acid catalysed cleavage of the different linkages in chitin with their respective rate constants used in our model. Two different rate constants are used for the hydrolysis of glycosidic linkages, depending on whether the preceding unit is an **A**-unit (k_{glycA}) or a **D**-unit (k_{glycD}) together with one rate constant

for the de-*N*-acetylation reaction (k_{acetyl}), assuming that k_{acetyl} is the same for all *N*-acetylated sugar units *i.e.* independent on chain lenght.

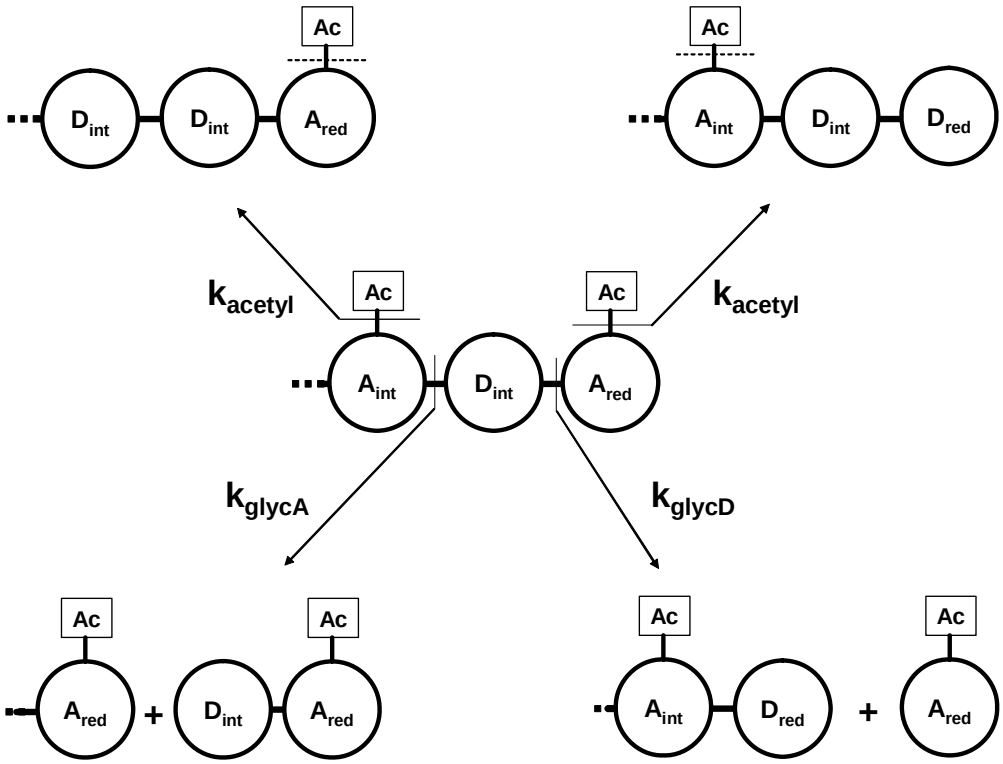

Figure 5.9 Schematic illustration of the acid catalysed cleavage of the different linkages present in chitin (shown as a polymer of **A**- and **D**-units).

From the four different sugar units, four different differential equations can be derived to express the change in the molar concentration as a function of time and rate constants. Table 5.1 shows the four equations expressing the molar concentrations of internal *N*-acetylated and de-*N*-acetylated sugar units ([$\mathbf{A_{int}}$] and [$\mathbf{D_{int}}$], respectively) and *N*-acetylated and de-*N*-acetylated reducing end sugar units ([$\mathbf{A_{red}}$] and [$\mathbf{D_{red}}$], respectively). From these equations (1-4), the theoretical molar fractions of each sugar unit can be determined as a function of time and rate constants.

Table 5.5 Theoretical model for the hydrolysis of chitin in concentrated acid. Equations expressing the molar concentrations of $\mathbf{A_{int}}$, $\mathbf{D_{int}}$, $\mathbf{A_{red}}$ and $\mathbf{D_{red}}$ as a function of time and the rate constants k_{acetyl}, k_{glycA} and k_{glycD}.

Eq. 1	$$[A_{int}](t) = [A_{int}]_0 \cdot e^{-t(k_{glycA}+k_{acetyl})}$$
Eq.2	$$[D_{int}](t) = e^{-t\cdot k_{glycD}} \cdot \left([D_{int}]_0 + \frac{k_{acetyl}\cdot[A_{int}]_0 \cdot (1-e^{-t(k_{glycA}+k_{acetyl}-k_{glycD})})}{k_{glycA}+k_{acetyl}-k_{glycD}}\right)$$
Eq.3	$$[A_{red}](t) = e^{-t\cdot k_{acetyl}}(1+[A_{int}]_0 - [A_{int}]_0 \cdot e^{-t\cdot k_{glycA}})$$
Eq. 4	$$[D_{red}](t) = \frac{(k_{glycD}-k_{glycA}-k_{acetyl})\cdot(1+[A_{int}]_0+[D_{int}]_0)-k_{acetyl}\cdot[A_{int}]_0\cdot e^{-t(k_{glycA}+k_{acetyl})}}{k_{glycD}-k_{glycA}-k_{acetyl}} -$$ $$\frac{(1+[A_{int}]_0)\cdot(k_{glycD}-k_{glycA}-k_{acetyl})\cdot e^{-t\cdot k_{acetyl}}}{k_{glycD}-k_{glycA}-k_{acetyl}} +$$ $$\frac{(k_{acetyl}([A_{int}]_0+[D_{int}]_0)-[D_{int}]_0(k_{glycD}-k_{glycA}))\cdot e^{-t\cdot k_{glycD}}}{k_{glycD}-k_{glycA}-k_{acetyl}}$$

5.3.2 Acid hydrolysis of chitin in concentrated DCl monitored by ^{1}H-NMR

The hydrolysis of chitin down to the end product glucosamine in concentrated DCl was monitored by ^{1}H-NMR. Figure 5.10 shows the ^{1}H-NMR-spectra of chitin in concentrated DCl as a function of time at 40°C.

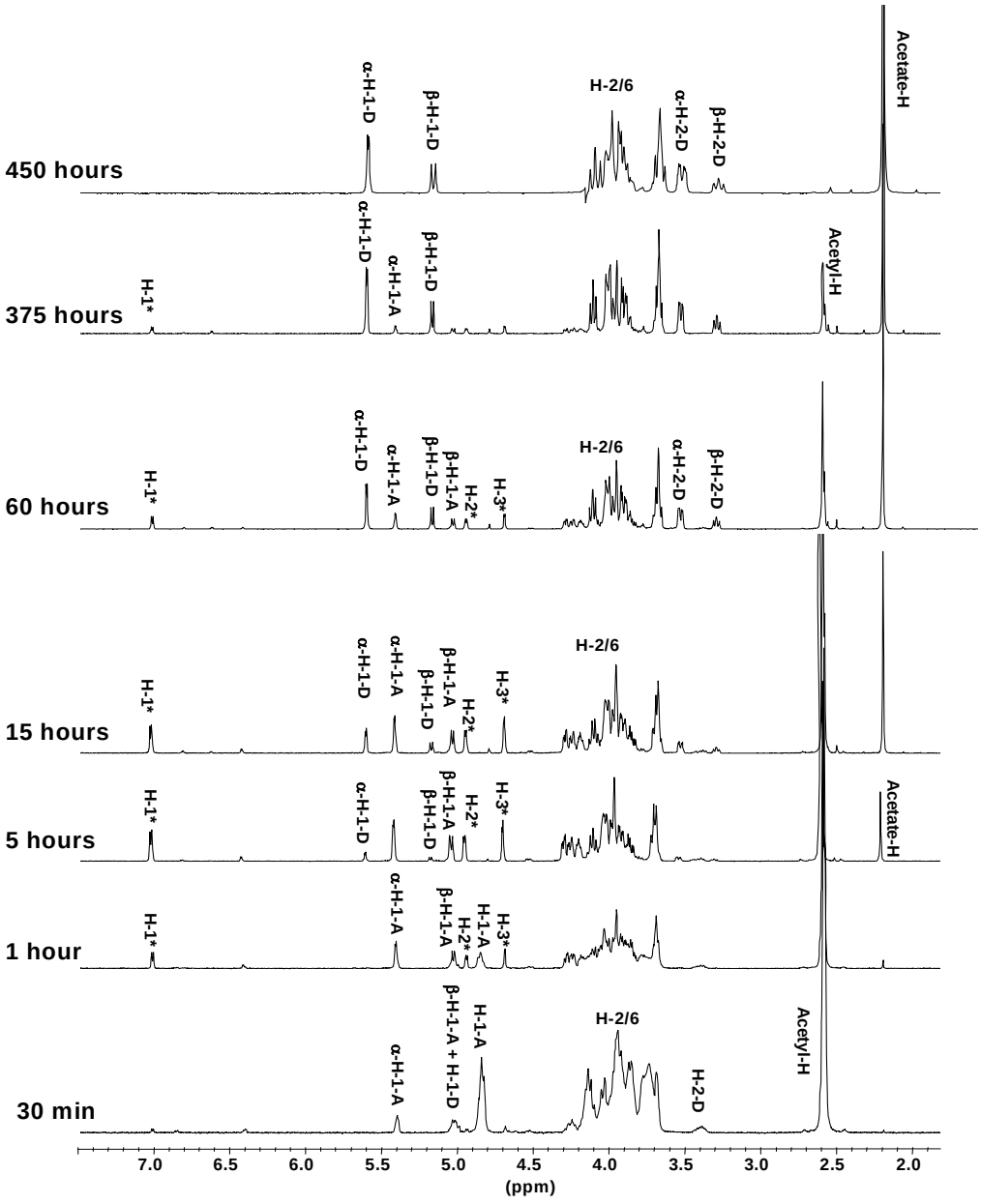

Figure 5.10 500 MHz ^{1}H-NMR spectra of chitin dissolved in concentrated DCl at 40°C (relative to resonance of TSP at 0.00 ppm). The resonance from H-1 of the glucofuranosyl oxazolinium ion is denoted with asterisk. Assignment of the resonances is discussed in Chapter 4.2.1 and Chapter 5.1.1.

From the increase in both the reducing end resonances and the acetic acid resonance in Figure 5.10, it can be concluded that the chitin chain is both depolymerised and de-*N*-acetylated. The formation of the monomer GlcNAc can be seen from the H-1 resonances of the glucofuranosyl oxazolinium ion (denoted with asterisk) which exists in

equilibrium with the monomer *N*-acetylglucosamine in concentrated DCl as described in Chapter 5.1.1. From the ^{1}H-NMR spectrum obtained after 30 minutes, the number average chain length (DPn) was found to be 24 units. The initial phase of the reaction (less than 5 hours) mainly results in depolymerisation of chitin to chitin oligomers and to the acetylated monomer, *N*-acetylglucosamine, which is subsequently de-*N*-acetylated to the monomer glucosamine. This is clearly seen from the relative intensities of the resonances from reducing end signals. After approximately 450 hours the chitin sample is fully de-*N*-acetylated to glucosamine.

5.3.3 Applying the model on experimental data

By integration of the different resonances from H-1 in the ^{1}H-NMR-spectra of Figure 5.10, we can obtain experimental values of the molar fraction of each of the four sugar units in a sample. Figure 5.11 shows the different theoretical and experimental molar fractions obtained from ^{1}H-NMR spectra of chitin dissolved in concentrated DCl at 40°C as a function of time. The continuous lines represent the optimal fit of the theoretical molar fractions from the model assuming an initial DP of 24 and using $k_{glycA} = 1.5 \cdot 10^{-4}\ s^{-1}$, $k_{glycD} = 1.3 \cdot 10^{-6}\ s^{-1}$ and $k_{acetyl} = 2.8. 10^{-6}\ s^{-1}$.

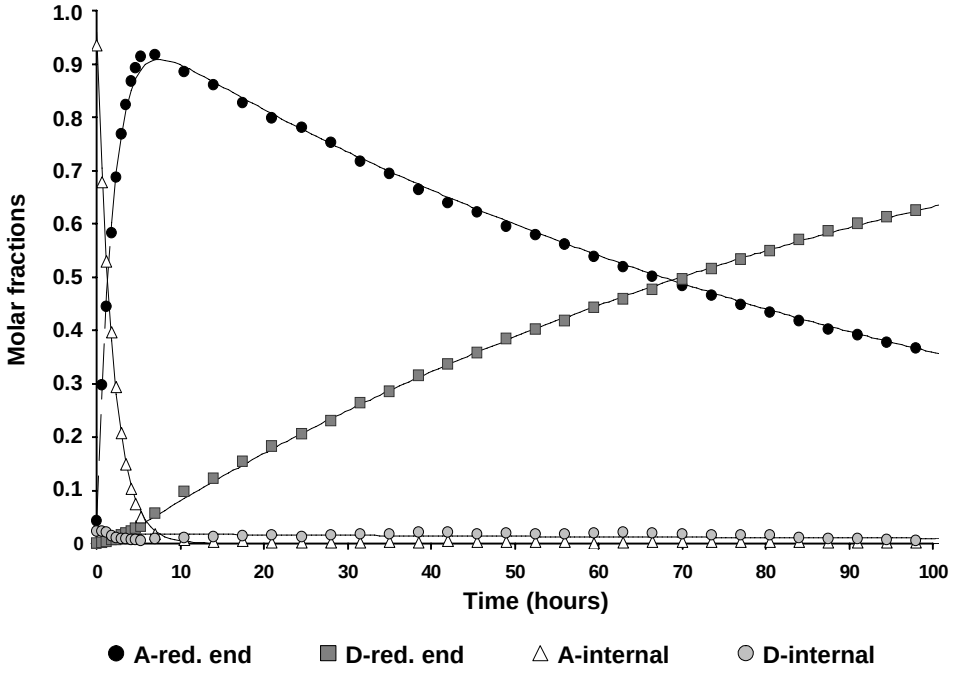

Figure 5.11 Molar fractions of the different sugar units as a function of time in a sample of chitin dissolved in concentrated DCl at 40 ° C (from Figure 5.10). Theoretical values for molar fractions are indicated by continuous lines (Using k_{glycA}= 1.5 · 10^{-4} s^{-1} and k_{glycD}= 1.3 · 10^{-6} s^{-1} and k_{acetyl}= 2.8 · 10^{-6} s^{-1}).

Figure 5.11 shows an excellent fit between the theoretical and experimental values when k_{glycA} is about 54 times higher than k_{acetyl} and 115 times higher than k_{glycD}. This is in accordance with our previously published results using chitin oligomers as model compounds to study the acid hydrolysis of chitin (Paper 4 and 5).

In order to more clearly see the details of the initial stages of the reactions, we expanded the first 10 hours of the chitin hydrolysis, which is shown in Figure 5.12. The results clearly show the rapid depolymerisation in the early stages of the reaction, showing the average chain length (DP_n) and the molar fractions of *N*-acetylated reducing ends ($\mathbf{A_{red}}$) and de-*N*-acetylated reducing ends ($\mathbf{D_{red}}$) as a function of time.

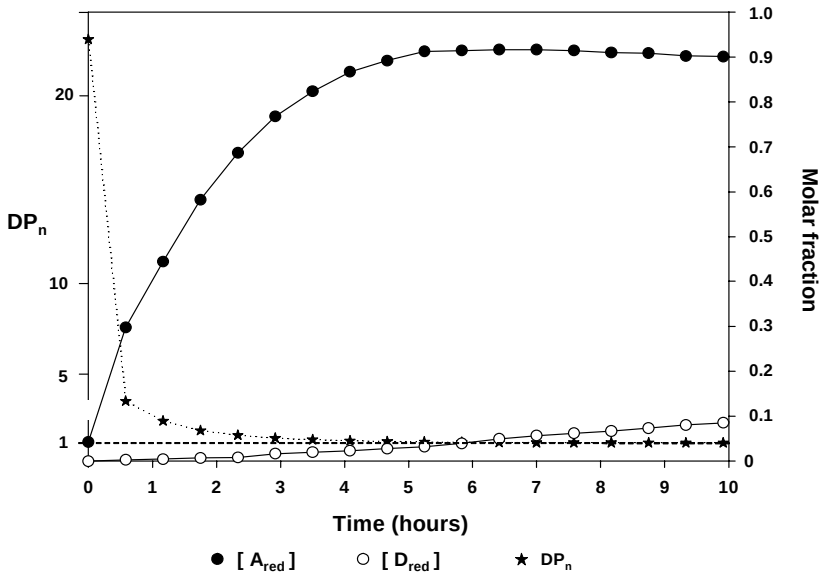

Figure 5.12 Experimental data of the number-average chain length (DP_n) and molar fractions of *N*-acetylated reducing ends ([$\mathbf{A}_{red}$]) and de-*N*-acetylated reducing ends ([$\mathbf{D}_{\mathbf{red}}$]) as a function of time.

The results show that DP_n decreases from 24 down to 1.0 during the first 6 hours, and the molar fraction of $\mathbf{A}_{\mathbf{red}}$ reaches a maximum of more than 0.9 after about 5 hours and then decreases almost linearly. This implies that the molar fraction of $\mathbf{A}_{\mathbf{red}}$ is almost exclusively composed of the monomer GlcNAc (in equilibrium with the glucosfuranosyl oxazolinium ion) around the maximum value of [$\mathbf{A}_{\mathbf{red}}$] (Figure 5.12). After 2 hours the DP_n levels out at 1.1 before decreasing to 1.0 after 6 hours. This means that the reaction mixture mainly consists of monomer and dimer during the time interval between 2 and 6 hours (a mixture of 90% monomer and 10% dimer would result in a DP_n of 1.1). It is likely that the dimer fraction present during the initial reaction mainly consist of the dimer **DA**, as the glycosidic linkage after a **D**-unit is hydrolysed at a much slower rate compared to the glycosidic linkage after an **A**-unit. The F_A of the chitin would be expected to be critical to the yield of the monomer GlcNAc, as an increasing content of single **D**-units in the chitin would result in the formation of increased amounts of the dimer **DA**. The assumption that k_{acetyl} is relatively independent of the chitin chain length is not critical as the de-*N*-acetylation reaction will almost exclusively occur at the reducing end when k_{glyc} is much larger than k_{acetyl}.

5.4 Concluding remarks

The difference in the rate of depolymerisation and de-*N*-acetylation of chitin in concentrated acid explains the reaction course seen in the hydrolysis of chitin in concentrated acid: since the depolymerization is much more rapid, deacetylation of polymeric units is insignificant in concentrated acid. Figure 5.13 illustrates the hydrolysis of chitin in concentrated acid.

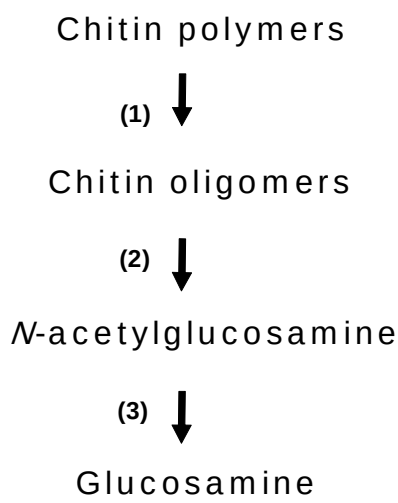

Figure 5.13 The hydrolysis of chitin in concentrated acid: (**1**) rapid degradation of the polysaccharide to smaller *N*-acetylated polymeric units, which are mainly (**2**) depolymerised to *N*-acetylglucosamine. (**3**) The more slow deacetylation of *N*-acetylglucosamine into glucosamine.

Our results indicate it is possible to produce *N*-acetylglucosamine in high yields by controlling the time and temperature of the reaction in Figure 5.13. A lower acid concentrations and/or a chitin starting material with a lower F_A could be predicted to lower the yield of *N*-acetylglucosamine, but could also render possible the production of other chitin oligomers by controlled acid hydrolysis.

SYMBOLS AND ABBREVIATIONS

α	Degree of scisson
α_s	Linear Expansion Factor
A_2	Second virial coefficient
ASSE	Absolute Sum of Squared Errors
C_∞	Characteristic ratio
COSY	Correlation NMR spectroscopy
DEPT	Disortionless Enhancement by Polarisation Transfer
DP	Degree of polymerisation
DP_n	Number average degree of polymerisation
F_A	Fraction of acetylated units
F_D	Fraction of deacetylated units
GlcN	Glucosamine
GlcNAc	*N*-acetyl-glucosamine
$g(\tau)$	Intensity autocorrelation function of the scattered light
HMQC	Heteronuclear Multiple Quantum Coherence
HSQC	Heteronuclear Single Quantum Coherence
k_b	Boltzmann's constant
L_c	Contour length
L_{mon}	Lenght of a projection of the repeating unit
M_n	Number-average molecular mass
M_W	Weight-average molecular mass
M_V	Viscosity average molecular weight
M_{mon}	Molecular weight of the repeating unit
MHS	Mark-Houwink-Sakurada
NMR	Nuclear Magnetic Resonance
N_A	Avogadro's number
N_k	Number of Kuhn statistical segments
$[\eta]$	Intrinsic viscosity
η_{rel}	Relative viscosity
η_{sp}	Specific viscosity
η_s	Solvent viscosity
Q_k	Length of Kuhn statistical segment
$\langle r^2_{e-e} \rangle$	Mean square end-to-end distance
R_G	Radius of gyration
R_H	Hydrodynamic radius
R_θ	Rayleigh ratio
RSSE	Relative Sum of Squared Errors
T	Absolute temperature

REFERENCES

1 Anderson J. W., Nicolosi R. J. and Borzelleca J. F. (2005). Glucosamine effects in humans: a review of effects on glucose metabolism, side effects, safety considerations and efficacy. *Food and Chemical Toxicology* **43**(2): 187-20

2 Anthonsen M. W., Vårum K. M., Hermansson A. M., Smidsrød O. and Brant D. A. (1994). Aggregates in Acidic Solutions of Chitosans Detected by Static Laser-Light Scattering. *Carbohydrate Polymers* **25**(1): 13-23.

3 Anthonsen M. W. & Smidsrød O. (1995). Hydrogen-Ion Titration of Chitosans with Varying Degrees of N-Acetylation by Monitoring Induced H-1-Nmr Chemical-Shifts. *Carbohydrate Polymers* **26**(4): 303-305.

4 Ballardie F. W., Capon B., Dearie W. M.. Foster R. L. (1976). Neighboring Acetamido-Group Participation in Reactions of Derivatives of 2-Acetamido-2-Deoxy-D-Glucose. *Carbohydrate Research* **49**: 79-92.

5 Bahrke S., Einarsson J.M., Gislason J., Haebel S., Peter-Katalinc J., Peter M.G. (2002). Characterization of chitooligosaccharides by mass spectrometry. Advances in Chitin Science, vol 6. (Ed. Vårum K.M.). Trondheim, Norway.

6 Baxter A., Dillon M., Taylor K.D.A., Roberts G.A.F. (1992). Improved Method for Ir Determination of the Degree of N-Acetylation of Chitosan. *International Journal of Biological Macromolecules* **14** (3): 166-169.

7 BeMiller J.N. (1965) In: *Starch*. Academic Press, New York. 495-499.

8 BeMiller J.N. (1967). Acid-catalyzed hydrolysis of glycosides. *Advances In Carbohydrate Chemistry And Biochemistry* **22**: 25-108.

9 Blackwel J., Parker K.D., Rudall K.M. (1967). Chitin Fibres of Diatoms Thalassiosira Fluviatilis and Cyclotella Cryptica. *Journal of Molecular Biology* **28**(2) : 383-388.

10 Blackwel J. (1969). Structure of Beta-Chitin or Parallel Chain Systems of Poly-Beta-(1-]4)-N-Acetyl-D-Glucosamine. *Biopolymers* **7** (3) :281-286.

11 Braconnot H. (1811). Sur la nature des champignons. *Ann. Chim.* (Paris) **79**: 265-304.

12 Båmstedt U. (1980). Biochemical components as indicators of seasonal conditions of deep-water zooplankton. In *Fjord Oceanography* (eds. H.J. Freeland, D.M. Farmer and C.D. Levings). Plenum Press, New York.

13 Carlstrom D. (1957). The Crystal Structure of Alpha-Chitin (Poly-N-Acetyl-D-Glucosamine). *Journal of Biophysical and Biochemical Cytology* **3**(5): 669-683.

14 Castle J.E, Deschamps J.R. & Tice K. (1984). In: *Chitin, Chitosan and Related Enzymes* (ed. Zikakis J.P.). Academic Press, London.

15 Clegg D.O., Reda D.J., Harris C.L., Klein M.A., O'Dell J.R., Hooper M.M., Bradley J.D., Bingham C.O., Weisman M.H., Jackson C.G., Lane N.E., Cush J.J., Moreland L.W., Schumacher H.R., Oddis C.V., Wolfe F., Molitor J.A., Yocum D.E., Schnitzer T.J., Furst D.E., Sawitzke A.D., Shi H., Brandt K.D., Moskowitz R.W., Williams H.J. (2006). Glucosamine, chondroitin sulfate, and the two in combination for painful knee osteoarthritis. *New England Journal of Medicine* **354** (8): 795-808.

16 D'Ambrosio B., Casa R., Bompani G., Scali M. (1981). Glucosamine sulfate: a controlled clinical investigation in arthrosis. *Pharmacotherpeutica* **2** : 504–508.

17 Darmon S.E. & Rudall K.M. (1950). Infra-Red and X-Ray Studies of Chitin. *Discussions of the Faraday Society* **9** : 251-260.

18 Deng M.D., Severson D.K., Grund A.D., Wassink S.L., Burlingame R.P., Berry A., Running J.A., Kunesh C.A., Song L., Jerrell T.A., Rosson R.A. (2005). Metabolic engineering of Escherichia coli for industrial production of glucosamine and N-acetylglucosamine. *Metabolic Engineering* **7**(3): 201-214.

19 Duarte M. L., Ferreira M. C., Marvao M. R. and Rocha J. (2001). Determination of the degree of acetylation of chitin materials by C-13 CP/MAS NMR spectroscopy. *International Journal of Biological Macromolecules* **28**(5): 359-363.

20 Duarte M.L., Ferreira M.C., Marvao M.R., Rocha J. (2002). An optimised method to determine the degree of acetylation of chitin and chitosan by FTIR spectroscopy. *International Journal of Biological Macromolecules* **31** (1-3): 1-8.

21 Edward J.T. (1955). Stability of glycosides to acid hydrolysis - A conformational analysis. *Chemistry and industry, **36**:* 1102-1104.

22 Falk M., Smith D. G., McLachla J. and McInnes A. G. (1966). Studies on Chitan (Beta-(1-]4)-Linked 2-Acetamido-2-Deoxy-D-Glucan) Fibers of Diatom Thalassiosira Fluviatilis Hustedt. *Canadian Journal of Chemistry* **44**(19): 2269-2281.

23 FDA (2006). US Food and Drug Administration Homepage, Office of Food Additive Safety; Summary of all GRAS notifications. http://www.cfsan.fda.gov/~rdb/opa-gras.html.

24 Flory P.J. (1953). Principles in polymer chemistry. Cornell University Press; New York.

25 Gatt R. & Berman E.R. (1966). A Rapid Procedure for Estimation of Amino Sugars on a Micro Scale. *Analytical Biochemistry* **15**(1): 167-172.

26 Giraud-Guille M. M., Bouligand Y. (1995). Crystal growth in a chitin matrix: the study of calcite development in the crab cuticle, in: Z.S. Karnicki et al. (Eds.), Chitin World, Wirtschaftsverlag: 136–144.

27 Giraud-Guille M. M. (1998). Plywood structures in nature. *Current Opinion in Solid State & Materials Science* **3** (3): 221-227.

28 Gooday G. W. (1990). The Ecology of Chitin Degradation. *Advances in Microbial Ecology* **11**: 387-430.

29 Hackman R.H. (1962). Studies on Chitin .5. Action of Mineral Acids on Chitin. *Australian Journal of Biological Sciences* **15** (3): 526-532.

30 Hackman R. H., Goldberg M. (1965). Studies on Chitin .6. Nature of Alpha- and Beta-Chitins. *Australian Journal of Biological Sciences* **18** (4): 935-941.

31 Hackman R.H. & Goldberg M. (1974). Light-Scattering and Infrared-Spectrophotometric Studies of Chitin and Chitin Derivatives. *Carbohydrate Research* **38** (1): 35-45.

32 Hai L., Diep T.B., Nagasawa N., Yoshii F., Kume T. (2003). Radiation depolymerization of chitosan to prepare oligomers. *Nuclear Instruments & Methods in Physics Research*, **208**: 466-470.

33 Haynes C.A., Aloise P., Creagh A.L. (1999). Process for producing N-acetyl-D-glucosamine. *United States Patent* 5,998,173.

34 He X.Y., Yin Q.R., Yang G.J. (2001). The production of *N*-acetyl-D-glucosamine. *J. Changde Teach. Univ. Nat. Sci.* **13**: 63-65.

35 Heux L., Brugnerotto J., Desbrieres J., Versali M. F. and Rinaudo M. (2000). Solid state NMR for determination of degree of acetylation of chitin and chitosan. *Biomacromolecules* **1**(4): 746-751.

36 Hirano, S. (1996). Chitin biotechnology applications. *Biotechnology Annual Review* **2**: 235–258.

37 Holan Z., Votruba J., Vlasakova V. (1980). New Method of Chitin Determination Based on Deacetylation and Gas-Liquid-Chromatographic Assay of Liberated Acetic-Acid. *Journal of Chromatography* **190** (1): 67-76.

38 Holme H. K., Foros H., Pettersen H., Dornish M. and Smidsrød O. (2001). Thermal depolymerization of chitosan chloride. *Carbohydrate Polymers* **46** (3): 287-294.

39 Horton D. & Lineback D.R. (1965). In: *Methods in Carbohydrate Chemsitry.* Academic Press. New York.

40 Hsiao H.Y., Tsai C.C., Chen S.M., Hsieh B.C., Chen R.L.C. (2004). Spectrophotometric determination of deacetylation degree of chitinous materials dissolved in phosphoric acid. *Macromolecular Bioscience* **4** (10): 919-921.

41 Hua, J., Suguro, S., Hirano, S., Sakamoto, K., Nagaoka, I. (2005). Preventive actions of a high dose of glucosamine on adjuvant arthritis in rats. *Inflammation Research* **54**(3):127-132.

42 Hungerford D.S., Jones L.C. (2003). Glucosamine and chondroitin sulfate are effective in the management of osteoarthritis. *Journal of Arthroplasty* **18** (3): 5-9

43 Kim S.K., Rajapakse N. (2005). Enzymatic production and biological activities of chitosan oligosaccharides (COS): A review. *Carbohydrate Polymers* **62**(4): 357-368.

44 Kozloff E. (1990). Invertebrates. Saunder College Publishing, New York.

45 Kumar M. N. V. R. (2000). A review of chitin and chitosan applications. *Reactive & Functional Polymers* **46** (1): 1-27.

46 Kroh L.W., Schulz A. (2001). News in the Maillard reaction of oligomeric carbohydrates: a survey. *Die Nahrung-Food* **45** (3): 160-163.

47 Maghami G.G. & Roberts G.A.F. (1988). Studies on the Adsorption of Anionic Dyes on Chitosan. *Makromolekulare Chemie-Macromolecular Chemistry and Physics* **189** (10) : 2239-2243.

48 Mathur N. K., Narang C. K. (1990). Chitin and Chitosan, Versatile Polysaccharides from Marine Animals. *Journal of Chemical Education* **67** (11): 938-942.

49 McCormick C. L., Callais P. A. and Hutchinson B. H. (1985). Solution Studies of Cellulose in Lithium-Chloride and N,N-Dimethylacetamide. *Macromolecules* **18**(12): 2394-2401.

50 MedlinePlus. (2006). U.S. National Library of Medicine and the National Institute of Healt. *http://www.nlm.nih.gov/medlineplus.*

51 Merzendorfer H. (2006). Insect chitin synthases: a review. Journal of *Comparative Physiology B-Biochemical Systemic and Environmental Physiology* **176** (1): 1-15.

52 Minke R., Blackwell J. (1978). Structure of Alpha-Chitin. *Journal of Molecular Biology* **120** (2): 167-181.

53 Mobasheri A., Vannucci S. J., Bondy C. A., Carter S. D., Innes J. F., Arteaga M. F., Trujillo E., Ferraz I., Shakibaei M., Martin-Vasallo P. (2002). Glucose transport and metabolism in chondrocytes: a key to understanding

chondrogenesis, skeletal development and cartilage degradation in osteoarthritis. *Histology and Histopathology* **17**(4): 1239-1267.

54 Moggridge R.C.G. & Neuberger A. (1938). *Journal of the Chemical Society* **745.**

55 Moore G.K. & Roberts G.A.F. (1977). In: Proceedings 1st International Conference on Chitin/Chitosan (Eds. Muzzarelli R.A.A. & Pariser E.R.). MIT Sea Grant Report 78-7, p 421.

56 Mustaparta E. (2006). Prices and market information on chitin products. Oral communication.

57 Muzzarelli R.A.A. (1977) Chitin. Pergamon Press, Oxford, Great Britain, 1-309.

58 Muzzarelli R.A.A. (1996). Chitosan-based dietary foods. *Carbohydrate Polymers* **29**: 309-316.

59 Ng C.H., Hein S., Chandrkrachang S. & Stevens W.F. (2006). Evaluation of an improved acid hydrolysis-HPLC assay for the acetyl content in chitin and chitosan. *Journal of Biomedical Materials Research Part B-Applied Biomaterials* **76B** (1): 155-160.

60 Novikov V.Y., Ivanov A.L. (1997). Synthesis of D(+)-glucosamine hydrochloride. *Russian Journal of Applied Chemistry* **70** (9): 1467-1470.

61 Pelletier A., Lemire I., Sygusch J., Chornet E., Overend R.P. (1990). Chitin Chitosan Transformation by Thermomechanochemical Treatment Including Characterization by Enzymatic Depolymerization. *Biotechnology and Bioengineering* **36**(3): 310-315.

62 Percot A., Viton C. and Domard A. (2003). Characterization of shrimp shell deproteinization. *Biomacromolecules* **4**(5): 1380-1385.

63 Percot A., Viton C. and Domard A. (2003). Optimization of chitin extraction from shrimp shells. *Biomacromolecules* **4**(1): 12-18.

64 Peter M.G., Kegel G., Keller R. (1986). Structural studies on sclerotized unsect cuticle, in: *Chitin in Nature and Technology* (eds. Muzarelli R.A.A., Jeuniaux C., Gooday G.W.). Plenum Press, New York.

65 Pettersen H., Sannes A., Holme H.K., Kristensen Å.H., Dornish M. & Smidsrød O. (2000). Thermal depolymerization of chitosan salts. In: *Advances in Chitin Science* **4** (Peter M.G., Domard A. & Muzzarelli R.A.A. eds.). University of Potsdam.

66 Piszkiewicz D. and Bruice T. (1967). Glycoside Hydrolysis. 1. Intramolecular Acetamido and Hydroxyl Group Catalysis in Glycoside Hydrolysis. *Journal of the American Chemical Society* **89**(24): 6237-6243.

67 Piszkiewicz D. and Bruice T. (1968). Glycoside Hydrolysis. 2. Intramolecular Carboxyl and Acetamido Group Catalysis in Beta-Glycoside Hydrolysis. *Journal of the American Chemical Society* **90**(8): 2156-2163.

68 Piszkiewicz D. and Bruice T. (1968). Glycoside Hydrolysis. 3. Intramolecular Acetamido Group Participation in the Specific Acid Catalyzed Hydrolysis of Methyl 2-Acetamido-2-deoxy-β-D-glucopyranoside. *Journal of the American Chemical Society* **90**(21): 5844-5848.

69 Poulicek M., Gaill F., Goffinet G. (1998). Chitin biodegradation in marine environments. *Nitrogen-containing macromolecules in the bio- and geosphere ACS symposium series* **707**: 163-210.

70 S. W. (1984). CONTIN (Version 2) Users manual; Technical Report EMBL-DA07. Max-Planck-Institut Biophysikalische Purves C.B. (1954). In: *Cellulose and Cellulose Derivatives*. Interscience Publishers. New York.

71 Purves C.B. (1954). In: *Cellulose and Cellulose Derivatives*. Interscience Publishers, New York.

72 Reginster, J. Y., Deroisy, R., Rovati, L. C., Lee, R. L., Lejeune, E., Bruyere, O., Giacovelli, G., Henrotin, Y., Dacre, J. E., Gossett, C. (2001). Long-term effects of glucosamine sulphate on osteoarthritis progression: a randomised, placebo-controlled clinical trial. *Lancet* **357**(9252):251-256.

73 Roberts G. A. F. (1992). Chitin Chemistry. The Macmillan Press Ltd.; London.

74 Rudall K. M. & Kenching W. (1973). Chitin System. *Biological Reviews of the Cambridge Philosophical Society* **48** (4): 597-605.

75 Rupley J. A. (1964). Hydrolysis of Chitin by Concentrated Hydrochloric Acid + Preparation of Low-Molecular-Weight Substrates for Lysozyme. *Biochimica Et Biophysica Acta* **83** (3): 245-251.

76 Saito H., Tabeta R. & Hirano S. (1982). A high resolution ^{13}C nmr study of chitin, chitosan and N-acyl chitosans by cross polarization/magic angle spinning (CP/MAS) nmr spectroscopy. Conformational behaviour and gelation mechanism. In: Chitin and Chitosan (Proceedings of the Second International Conference on Chitin and Chitosan), eds. S. Hirano & S. Tokura, Sapporo, Japan. 71-76.

77 Sandford P. A. (2002). Commercial sources of chitin & chitosan and their utilization. Advances in Chitin Science, vol 6. (Ed. Vårum K.M.). Trondheim, Norway.

78 Sannan T., Kurita K. and Iwakura Y. (1976). Studies on Chitin 2. Effect of Deacetylation on Solubility. *Makromolekulare Chemie-Macromolecular Chemistry and Physics* **177**(12): 3589-3600.

79 Sannan T., Kurita K. and Iwakura Y. (1977). Studies on Chitin 5. Kinetics of Deacetylation Reaction. *Polymer Journal* **9**(6): 649-651.

80 Saito H., Tabeta R., Hirano S. (1982). A high resolution 13C nmr study of chitin, chitosan and N-acyl chitosans by cross polarization/magic angle spinning (CP/MAS) nmr spectroscopy. Conformational behaviour and gelation mechanism. In: *Chitin and Chitosan* (Proceedings of the Second International Conference on Chitin and Chitosan), eds. S. Hirano & S. Tokura, Sapporo, Japan: 71-76.

81 Sato H., Mizutani S., Tsuge S., Ohtani H., Aoi K., Takasu A., Okada M., Kobayashi S., Kiyosada T., Shoda S. (1998). Determination of the degree of acetylation of chitin/chitosan by pyrolysis gas chromatography in the presence of oxalic acid. *Analytical Chemistry* **70** (1): 7-12.

82 Smidsrød O. and Moe S.T. (1995). Biopolymerkjemi. Tapir Forlag, Trondheim.

83 Stryer L. (1995). Biochemistry 4th ed. W.H. Freeman and Company, New York.

84 Tanford C. (1961). Physical Chemistry of Macromolecules. John Wiley; New York.

85 Tanner S.F., Chanzy H., Vincendon M., Roux J.C., Gaill F. (1990). High-Resolution Solid-State C-13 Nuclear-Magnetic-Resonance Study of Chitin. *Macromolecules* **23** (15): 3576-3583.

86 Terbojevich M., Carraro C., Cosani A. and Marsano E. (1988). Solution Studies of the Chitin Lithium Chloride-N,N-Dimethylacetamide System. *Carbohydrate Research* **180**(1): 73-86.

87 Urbanczyk G., Lipp A., Symonowicz B., Szosland I., Jeziorny A., Urbaniak J., Domagala W., Dorau K., Wrzosek H., Sztajnowski S., Kowalska S., Sztajnert E. (1997). Chitin filaments from dibutyrylchitin precursor: Fine structure and physical and physicochemical properties. *Journal of Applied Polymer Science* **65** (4): 807-819.

88 US Patent and Trademark Office (2006). Homepage: http://www.uspto.gov/patft/index.html.

89 Vårum K. M., Anthonsen M. W., Grasdalen H. and Smidsrød O. (1991). High-Field Nmr-Spectroscopy of Partially N-Deacetylated Chitins (Chitosans) 1. Determination of the Degree of N-Acetylation and the Distribution of N-Acetyl Groups in Partially N-Deacetylated Chitins (Chitosans) by High-Field Nmr-Spectroscopy. *Carbohydrate Research* **211**(1): 17-23.

90 Vårum, K. M., M. W. Anthonsen, H. Grasdalen and O. Smidsrød (1991). ^{13}C-N.m.r. studies of the acetylation sequences in partially *N*-deacetylated chitins (chitosans). *Carbohydrate Research* **217**: 19-27.

91 Vårum K.M., Holme H.K., Izume M., Stokke B.T., Smidsrød O. (1996). Determination of enzymatic hydrolysis specificity of partially N-acetylated chitosans. *Biochimica Et Biophysica Acta-General Subjects* **1291** (1): 5-15.

92 Vårum K. M., Ottøy M. H. and Smidsrød O. (2001). Acid hydrolysis of chitosans. *Carbohydrate Polymers* **46**: 89-98.

93 Wiberg, K. B. (1955). The Deuterium Isotope Effect. *Chemical Reviews* **55** (4): 713-743.

94 Weintraub M. & French D. (1970). Acid Hydrolysis of (1-4)-Alpha-D-Glucans. Analysis of Products by Quantitative Paper Chromatography. *Carbohydrate Research* **15** (2): 241-250.

95 Yamakawa H. & Fujii M. (1974). Light-Scattering from Wormlike Chains - Determination of Shift Factor. *Macromolecules* **7** (5): 649-654.